# N–O Bond Activation and Cleavage Reactions of the Nitrosyl-Bridged Complexes $[M_2Cp_2(\mu\text{-}PCy_2)(\mu\text{-}NO)(NO)_2]$ (M = Mo, W).

M. Angeles Alvarez, M. Esther García, Daniel García-Vivó,* Alberto Ramos, Miguel A. Ruiz,* and Adrián Toyos.

*Departamento de Química Orgánica e Inorgánica/IUQOEM, Universidad de Oviedo, E-33071 Oviedo, Spain.*

## Abstract

The title complexes (**1a,b**) were prepared in two steps by first reacting the hydrides $[M_2Cp_2(\mu\text{-}H)(\mu\text{-}PCy_2)(CO)_4]$ with $[NO](BF_4)$ in the presence of $Na_2CO_3$ to give dinitrosyls $[M_2Cp_2(\mu\text{-}PCy_2)(CO)_2(NO)_2](BF_4)$, which were then fully decarbonylated upon reaction with $NaNO_2$ at 323 K. An isomer of the $Mo_2$ complex having a cisoid arrangement of the terminal ligands (***cis*-1a**) was prepared upon irradiation of toluene solutions of **1a** with visible-UV light at 288 K. The structure of these trinitrosyl complexes was investigated using X-ray diffraction and density functional theory (DFT) calculations, these revealing a genuine pyramidalization of the bridging NO that might be associated in part to an increase of charge at the N atom, and also anticipated a weakening of the N–O bond upon reaction with bases or reducing reagents. Complexes **1a,b** reacted with $[FeCp_2](BF_4)$ to give first the radicals $[M_2Cp_2(\mu\text{-}PCy_2)(\mu\text{-}NO)(NO)_2](BF_4)$ according to CV experiments, which then underwent H-abstraction to yield the nitroxyl-bridged complexes $[M_2Cp_2(\mu\text{-}PCy_2)(\mu\text{-}\kappa^1\text{:}\eta^2\text{-}HNO)(NO)_2](BF_4)$, alternatively prepared upon protonation with $HBF_4{\cdot}OEt_2$. The novel coordination mode of the nitroxyl ligand in these products was thermodynamically favored over its tautomeric hydroximido form, according to DFT calculations, and similar nitrosomethane-bridged cations $[M_2Cp_2(\mu\text{-}PCy_2)(\mu\text{-}\kappa^1\text{:}\eta^2\text{-}MeNO)(NO)_2]^+$ were prepared by reacting **1a,b** with $CF_3SO_3Me$ or $[Me_3O]BF_4$. Complexes **1** reacted with M(Hg) (M = Zn, Na) in tetrahydrofuran to give the amido-bridged derivatives $[M_2Cp_2(\mu\text{-}PCy_2)(\mu\text{-}NH_2)(NO)_2]$ with retention of stereochemistry, a transformation also induced by using mild O-atom scavengers such as CO and phosphites in the presence of water. In the absence of water, phosphites accomplished a deoxygenation of the bridging NO of the $Mo_2$ complexes to yield the phosphoraniminato-bridged derivatives $[Mo_2Cp_2(\mu\text{-}PCy_2)\{\mu\text{-}NP(OR)_3\}(NO)_2]$ (R = Et, Ph), also with retention of stereochemistry.

# Introduction

Nitric oxide is a fascinating and multifunctional molecule. From the inorganic chemist's point of view, this stable radical can be qualified as an excellent and versatile ligand which can strongly bind transition-metal atoms in both high and low oxidation states while adopting many different coordination modes, to give a plethora of coordination and organometallic nitrosyl complexes ranging from mononuclear to cluster species with interesting stoichiometric and catalytic reactivity.[1] From a more applied point of view, this molecule can be viewed as a sort of Janus-faced species, with both beneficial and undesirable effects, but in any case control of these effects often involves the interaction of NO with metal centers in one or another way. On one side, nitric oxide has a relevant and diverse biological activity (neurotransmission, blood pressure regulation, nitrification and denitrification processes, etc) which depends, *inter alia*, on its interaction with transition-metal centers,[1,2] while some nitrosyl complexes can be even designed to release NO in a controlled way within living organisms for therapeutic purposes.[3] On the other side, nitric oxide itself is one of the most important atmospheric pollutants requiring metal-mediated catalytic abatement,[1,4,5] and the study of metal-nitrosyl interactions can therefore lead to the design of more efficient and sustainable catalysts for the removal of this pollutant (usually by reduction). In all, many of the above transformations involve at some critical stage the metal-mediated cleavage of a N–O bond. Thus, the activation and cleavage of the strong N–O bond of nitric oxide when bound to a metal centre has long been a matter of interest in the field of inorganic chemistry. However, most of the research on nitrosyl complexes has been developed so far on mononuclear species, while the chemistry of binuclear complexes remains comparatively less explored, particularly in the case of polynitrosyl complexes, even if these substrates might be well suited for nitrosyl activation in a number of ways, thanks to the cooperative action of two close metal centers. Some relevant examples of NO activation and eventual cleavage at well-defined binuclear polynitrosyl complexes include N–O bond oxidative addition at $Mo_2$ centers,[6] reduction to a $\mu$-$NH_2$ ligand at $Cr_2$ or $Co_2$ centers,[7] and reductive coupling to $\mu$-$N_2O_2$ at $Ru_2$ centers, with eventual release of $N_2O$ in the presence of acids,[8] or upon photochemical activation.[9] We finally note that some examples of nitrosyl N–O bond cleavage at polynuclear clusters have been also documented.[10]

**Chart 1**

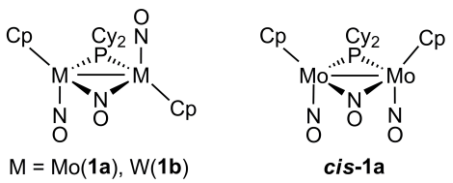

In a preliminary study on metal-mediated NO activation, we recently implemented a convenient preparation for the trinitrosyl complex $[Mo_2Cp_2(\mu\text{-}PCy_2)(\mu\text{-}NO)(NO)_2]$ (**1a**), a molecule displaying a bridging nitrosyl ligand with significant pyramidalization at the N atom (Chart 1; Cp = $\eta^5$-$C_5H_5$), which turned to undergo interesting transformations under mild conditions, such as protonation at the N site, easy reduction to $NH_2$ and deoxygenation by $P(OPh)_3$.[11] In order to gain more insight into these unusual transformations, we have now analyzed in more detail the structure, acid-base and redox behavior of the above complex, a study which we have also extended to its ditungsten analogue $[W_2Cp_2(\mu\text{-}PCy_2)(\mu\text{-}NO)(NO)_2]$ (**1b**) and a structural isomer featuring a cisoid arrangement of the MoCp(NO) fragments (***cis*-1a**, Chart 1), so as to ponder the influence of metal and overall stereochemistry on the structure and reactivity of the distorted bridging nitrosyl in these substrates. As it will be shown below, both factors have a significant influence both on the pyramidalization of the bridging nitrosyl in these substrates and on their chemical behavior.

## Results and Discussion

**Synthesis of Trinitrosyl Complexes 1.** In our preliminary study, we found that the dimolybdenum complex **1a** could be conveniently prepared in a two-step process which starts with the reaction of the hydride $[Mo_2Cp_2(\mu\text{-}H)(\mu\text{-}PCy_2)(CO)_4]$ in dichloromethane solution with two equiv of $[NO]BF_4$, in the presence of excess sodium carbonate to remove the hydride ligand (otherwise reaction never goes to completion).[11] This accomplishes a CO by $NO^+$ substitution and deprotonation, to give the corresponding cationic dinitrosyl complex $[Mo_2Cp_2(\mu\text{-}PCy_2)(CO)_2(NO)_2](BF_4)$ (**2a**) in high yield. In the second stage, the latter product is fully decarbonylated upon reaction with $NaNO_2$ in tetrahydrofuran at 323 K to eventually give **1a**, a product isolated in 63% yield after chromatographic workup (Scheme 1), thus drastically improving an earlier, low-yield preparation of this complex.[12] The reaction of carbonyl complexes with nitrite salts is one of the general synthetic routes to organometallic nitrosyl complexes, a process resulting in O-atom transfer from nitrite to a carbonyl ligand, which is then released as $CO_2$.[1] This process may involve direct nucleophilic attack of the nitrite anion to the C atom of a carbonyl ligand or, alternatively, prior coordination of nitrite to give an intermediate nitrito complex which then undergoes intramolecular O-transfer to a metal-bound carbonyl, as found recently by us in the case of the ditungsten complex $[W_2Cp_2(\mu\text{-}PPh_2)_2(\kappa^1\text{-}ONO)(CO)(NO)]$.[13]

The above two-step procedure also works efficiently for the related ditungsten complex $[W_2Cp_2(\mu\text{-}H)(\mu\text{-}PCy_2)(CO)_4]$,[14] which thus is similarly converted into the new trinitrosyl complex $[W_2Cp_2(\mu\text{-}PCy_2)(\mu\text{-}NO)(NO)_2]$ (**1b**) *via* the cationic intermediate $[W_2Cp_2(\mu\text{-}PCy_2)(CO)_2(NO)_2](BF_4)$ (**2b**). Complex **1b** turned out to be less stable than

its dimolybdenum analogue, actually decomposing in part during chromatographic workup even at 253 K, with all of it posing some restrictions to the study of its reactivity. We finally note that, although both trinitrosyls **1a** and **1b** are obtained as single isomers, the corresponding cationic intermediates **2a,b** are formed as a mixture of two isomers in each case, a matter to be discussed below.

**Scheme 1. Preparation of Trinitrosyl Complexes 1**

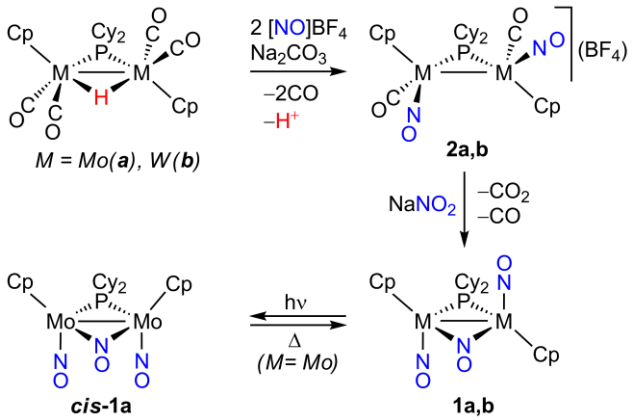


As a part of the general study on the chemical behavior of trinitrosyls **1a,b** we first examined their thermal and photochemical stability, and found substantial differences between the dimolybdenum and ditungsten complexes. Thus, the dimolybdenum compound **1a** experienced no significant transformation in refluxing toluene solution for a few hours, whereas the ditungsten analogue **1b** underwent full decomposition under the same conditions, with no intermediate complexes being detected along the process. Full decomposition was also observed upon irradiation of toluene solutions of **1b** with visible-UV light at room temperature. In contrast, a similar photochemical treatment of the dimolybdenum complex **1a** caused its selective rearrangement into the corresponding isomer displaying a cisoid disposition of both MoCp(NO) fragments (***cis*-1a**, Scheme 1). Compound ***cis*-1a** is thermodynamically less stable than its transoid isomer **1a** (see below) and, while stable in solution at room temperature, it can be fully converted back to **1a** by refluxing its toluene solutions for 3 h.

**Structural Characterization of Dinitrosyl Precursors 2.** As noticed above, the cationic complexes **2a,b** are obtained as a mixture of two isomers (**A** and **B**) in each case, as indicated by the observation of separated $^{31}P$ and $^{1}H$ NMR resonances, and even of different C–O and N–O stretches (Table 1 and Experimental Section). The relative **A**/**B** ratio of isomers changes with solvent, and it was measured to be ca. 4/1 (Mo) and 5/1 (W) in $CD_2Cl_2$ solution, but it was lower in tetrahydrofuran solution. The major isomer **A** in each case displays equivalent MCp(NO)(CO) fragments, as denoted by the observation of a single Cp resonance for both **2a** and **2b**, and identical $^{31}P$–$^{183}W$ couplings of 183 Hz for the phosphanyl ligand to both metal atoms in the case of **2b**. This isomer is then assumed to have the transoid structure depicted in Chart 2, with both

nitrosyl ligands *trans* to the $PCy_2$ bridge, as determined crystallographically for the related $PPh_2$-bridged complex $[Mo_2Cp_2(\mu\text{-}PPh_2)(CO)_2(NO)_2](BF_4)$.[15] In contrast, the minor isomers **B** display two distinct Cp resonances in each case, while the tungsten complex displays quite different P–W couplings of 177 and 294 Hz, which can be only explained by assuming a change of the ligand positioned *trans* to P (CO instead of NO) at one of the metal fragments (Chart 2).[16] Spectroscopic differences between compounds **2a** and **2b** are the expected ones when comparing Mo and W complexes (higher C–O and N–O stretches, and substantially higher $^{31}P$ chemical shifts for the molybdenum complexes),[14] and deserve no further comments.

**Table 1.** Selected IR,[a] and $^{31}P\{^1H\}$ Data[b] for New Compounds.

| Compound | $\nu$(NO) | $\delta$(P) [$J_{PW}$] |
|---|---|---|
| $[Mo_2Cp_2(\mu\text{-}PCy_2)(\mu\text{-}NO)(NO)_2]$ (**1a**)[c] | 1625 (w, sh), 1587 (vs)[d] | 219.4 |
| $[W_2Cp_2(\mu\text{-}PCy_2)(\mu\text{-}NO)(NO)_2]$ (**1b**) | 1611 (w), 1568 (vs)[e] | 143.5 [340] |
| *cis*-$[Mo_2Cp_2(\mu\text{-}PCy_2)(\mu\text{-}NO)(NO)_2]$ (***cis*-1a**) | 1645 (vs), 1583 (m)[f] | 221.5 |
| $[Mo_2Cp_2(\mu\text{-}PCy_2)(CO)_2(NO)_2](BF_4)$ (**2a**) | 1679 (vs) | 279.8 (isomer **A**)<br>276.6 (isomer **B**)[g] |
| $[W_2Cp_2(\mu\text{-}PCy_2)(CO)_2(NO)_2](BF_4)$ (**2b**) | 1665 (vs) | 204.0 [183] (isomer **A**)<br>190.8 [293, 177] (isomer **B**)[h] |
| $[Mo_2Cp_2(\mu\text{-}PCy_2)(\mu\text{-}\kappa^1\text{:}\eta^2\text{-}HNO)(NO)_2](BF_4)$ (**3a**) | 1689 (m, sh), 1662 (vs) | 258.1 |
| $[W_2Cp_2(\mu\text{-}PCy_2)(\mu\text{-}\kappa^1\text{:}\eta^2\text{-}HNO)(NO)_2](BF_4)$ (**3b**) | 1668 (m, sh), 1640 (vs) | 167.0 [312, 222] |
| $[Mo_2Cp_2(\mu\text{-}PCy_2)(\mu\text{-}\kappa^1\text{:}\eta^2\text{-}MeNO)(NO)_2](BAr'_4)$ (**4a**) | 1677 (m, sh), 1662 (vs) | 256.7 (isomer **A**)<br>251.1 (isomer **B**)[i] |
| $[W_2Cp_2(\mu\text{-}PCy_2)(\mu\text{-}\kappa^1\text{:}\eta^2\text{-}MeNO)(NO)_2](CF_3SO_3)$ (**4b**) | 1658 (m, sh), 1639 (vs) | 167.3 [311, 220] (isomer **A**)<br>157.2 (isomer **B**)[j] |
| $[Mo_2Cp_2(\mu\text{-}PCy_2)(\mu\text{-}NH_2)(NO)_2]$ (**5a**) | 1580 (w, sh), 1553 (vs) | 208.7 |
| $[W_2Cp_2(\mu\text{-}PCy_2)(\mu\text{-}NH_2)(NO)_2]$ (**5b**) | 1542 (vs) | 135.1 [363] |
| *cis*-$[Mo_2Cp_2(\mu\text{-}PCy_2)(\mu\text{-}NH_2)(NO)_2]$ (***cis*-5a**) | 1594 (vs), 1556 (m) | 214.9 |
| $[Mo_2Cp_2(\mu\text{-}PCy_2)\{\mu\text{-}NP(OEt)_3\}(NO)_2]$ (**6**) | 1560 (w, sh), 1534 (vs) | 215.3 ($\mu$-P), 26.9 (NP) |
| $[Mo_2Cp_2(\mu\text{-}PCy_2)\{\mu\text{-}NP(OPh)_3\}(NO)_2]$ (**7**) | 1560 (w, sh), 1543 (vs) | 218.2 ($\mu$-P), 5.2 (NP) |
| *cis*-$[Mo_2Cp_2(\mu\text{-}PCy_2)\{\mu\text{-}NP(OPh)_3\}(NO)_2]$ (***cis*-7**) | 1580 (vs), 1545 (m) | 223.0 ($\mu$-P), –2.3 (NP) |

[a] Recorded in dichloromethane solution, with N–O stretching bands [$\nu$(NO)] in $cm^{-1}$. [b] Recorded in $CD_2Cl_2$ solution at 121.49 MHz and 293 K, with chemical shifts ($\delta$) in ppm and $^{31}P$-$^{183}W$ couplings ($J_{PW}$) in Hz. [c] Data taken from reference 12. [d] $\nu$(NO) = 1589 (vs), 1420 (m) in KBr pellet. [e] $\nu$(NO) = 1616 (m), 1566 (vs), 1360 (w) in KBr pellet. [f] $\nu$(NO) = 1643 (vs), 1581 (s), 1393 (m) in KBr pellet. [g] Ratio **A**/**B** = 4. [h] Ratio **A**/**B** = 5. [i] Ratio **A**/**B** = 2. [j] Ratio **A**/**B** = 3.5.

## Chart 2. Solution Isomers of Complexes 2a,b

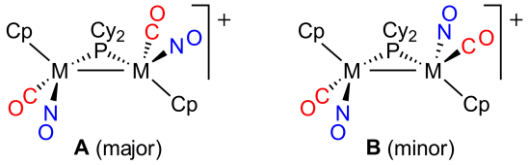

**Structure of Trinitrosyl Complexes 1.** The structure of **1a** in the solid state was determined in our preliminary study on this chemistry.[11] We have now determined the structure of its isomer ***cis*-1a** (Figure 1), and that of its ditungsten analogue **1b** (Figure S1). A selection of the structural parameters of these three complexes is collected in Table 2.

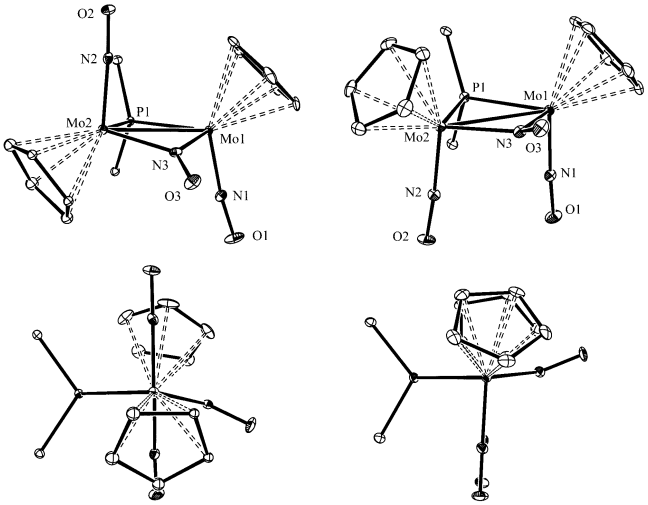


**Figure 1**. ORTEP diagram (30% probability) of compounds **1a** (left)[11] and ***cis*-1a** (right, only one of the two independent molecules shown), with H atoms and Cy groups (except their $C^1$ atoms) omitted for clarity. Below, the corresponding projections along the Mo–Mo bonds are shown.

**Table 2.** Selected Bond Lengths (Å) and Angles (º) for Compounds**1**

| parameter | **1a**[a] | ***cis*-1a** | ***cis*-1a** (2)[b] | **1b** |
|---|---|---|---|---|
| M1–M2 | 2.8935(3) | 2.9234(8) | 2.9280(8) | 2.907(2) |
| M1–P1 | 2.4063(7) | 2.421(2) | 2.419(2) | 2.441(7) |
| M2–P1 | 2.4155(7) | 2.417(2) | 2.426(2) | 2.437(7) |
| M1–N3 | 2.031(2) | 2.020(6) | 2.027(5) | 2.07(2) |
| M2–N3 | 2.018(2) | 2.027(5) | 2.024(6) | 2.03(2) |
| M1–N1 | 1.784(2) | 1.794(6) | 1.800(6) | 1.75(2) |
| M2–N2 | 1.798(2) | 1.792(5) | 1.798(6) | 1.73(2) |
| N3–O3 | 1.227(3) | 1.240(6) | 1.240(7) | 1.20(3) |
| M1–P1–M2 | 73.75(2) | 74.36(5) | 74.37(5) | 73.2(2) |
| M1–N3–M2 | 91.2(1) | 92.5(2) | 92.6(2) | 90.5(8) |
| M1–M2–N2 | 88.9(1) | 94.8(2) | 93.7(2) | 82.0(1) |
| M2–M1–N1 | 105.4(1) | 93.2(2) | 94.3(2) | 111.9(1) |
| M1–N3–O3 | 131.8(2) | 132.2(4) | 131.8(5) | 132(2) |
| M2–N3–O3 | 134.5(2) | 130.4(5) | 131.6(5) | 134(2) |
| $\Sigma$(N3)[c] | 357.5 | 355.1 | 356.0 | 356.5 |
| $\alpha$(*pd*)[d] | 167.8 (0.22) | 162.5 (0.32) | 164.3 (0.29) | 166.6 (0.24) |
| $\beta$[e] | 164.4 | 176.5 | 178.5 | 157.3 |

[a] Data taken from reference 11. [b] Data for the second independent molecule present in the unit cell. [c] Summation of bond angles around N3. [d] Angle ($\alpha$) defined by the bridging NO ligand and the centroid (ct) of the M–M bond; the pyramidalization degree (*pd*) of the bridging NO ligand is defined as (180-$\alpha$)/54.75 (see text). [e] Folding angle of the central MPMN skeleton, defined by the P1–ct–N3 or P–M–M–N3 angles.

All these molecules are built from MCp(NO) fragments bridged symmetrically by $PCy_2$ (M–P 2.41-2.44 Å) and NO ligands (M–N 2.02-2.07 Å). In isomer ***cis*-1a** the

terminal Cp and NO ligands adopt an eclipsed conformation leaving the latter ligands almost parallel to each other, and the central MoPMoN skeleton is almost flat, with a folding angle close to 180º ($\beta$ in Table 2). In the transoid isomers **1a** and **1b** the terminal nitrosyls are arranged in a distorted antiparallel fashion, with a nitrosyl ligand defining a M–M–NO angle slightly below 90º and the second one pointing away from the dimetal center (M–M–NO > 105º), and all of this is accompanied by a substantial folding of the central M–P–M–N skeleton, with $\beta$ angles of ca. 164 (Mo) and 157º (W). We have recently found a similar structural distortion in the isoelectronic carbyne complex $[W_2Cp_2(\mu\text{-}PCy_2)(\mu\text{-}CNH^tBu)(NO)_2]$,[17] which there we attributed to steric effects derived from the presence of the bulky carbyne group, but obviously this cannot be the case of the nitrosyl-bridged compounds **1a,b**; here, electronic factors are likely responsible for the observed folding of the central skeleton, which would be higher for the complex bearing the electron richer metal center (W, instead of Mo atoms). Overall, compounds **1** are 34-electron complexes, for which a metal–metal single bond has to be formulated according to the 18-electron rule; this is consistent with the intermetallic lengths of 2.89-2.93 Å found in these molecules, actually quite similar to that measured in the mentioned carbyne-bridged complex (2.9010(4) Å).

The most remarkable structural feature of complexes **1**, however, is the significant pyramidalization (instead of the expected trigonal planar environment) observed at the N atom of the bridging nitrosyl ligand, which has no obvious origin. In a complex having a roughly symmetrical bridging nitrosyl, this effect can be conveniently quantified through the angle defined by the bridging NO ligand and the centroid (ct) of the M–M bond ($\alpha$ in Table 2). Such an angle would have a value of 180º for a planar trigonal environment of the N atom, and 125.25º for an ideal tetrahedral environment.[18] Thus we can define the pyramidalization degree (*pd*) through equation 1, which would render extreme *pd* values of 0 and 1 for ideal planar trigonal and tetrahedral environments, respectively.

$$pd = (180-\alpha)/(180-125.25) \qquad \text{(eq. 1)}$$

For compounds **1**, the pyramidalization degree of the bridging nitrosyl follows the order **1a** (0.22) < **1b** (0.24) < ***cis*-1a** (0.30). A search at the Cambridge Crystallographic Data Centre database reveals that only six other complexes have been found previously with such a strong departure of a bridging nitrosyl away from a planar environment (5 examples with $pd \approx 0.22$,[7b,19] and just one example with $pd = 0.30$),[20] but no attention seems to have been paid to it. In a series of complexes $[Ru_2(CO)_4(\mu\text{-}NO)(\mu\text{-}P^tBu_2)(\mu\text{-}R_2PCH_2PR_2)]$ structurally characterized,[19d] we notice that the pyramidalization degree of the bridging NO is only moderately sensitive to the nature of the R groups in the bridging diphosphine, it increasing in the sequence Cy (0.16) < Ph (0.19) < Me (0.22). Interestingly, the related cation $[Ru_2(CO)_4(\mu\text{-}H)(\mu\text{-}NO)(\mu\text{-}P^tBu_2)(\mu\text{-}Me_2PCH_2PMe_2)]^+$

displayed an almost conventional nitrosyl ligand (*pd* = 0.06).[21] From all of this we conclude that, for complexes having the same overall structure, more electron density at the dimetal center might favor a larger pyramidalization at the bridging nitrosyl, with steric effects possibly playing only a minor role. This is in agreement with the observation of higher *pd* value for the ditungsten complex **1b**, when compared to the dimolybdenum analogue **1a**, although the lower precision of the structural data for **1b** precludes a more detailed analysis of these figures. In any case, we have further addressed this matter in the light of density functional theory (DFT) calculations on these three complexes (see below).

Spectroscopic data for compounds **1** in solution (Table 1 and Experimental Section) are fully consistent with the structures found in the solid state, and support their retention in solution. The transoid isomers **1a** and **1b** expectedly give rise to two N–O stretches for the terminal nitrosyls, with weak and strong intensity in order of decreasing frequency, as found for related $M_2(CO)_2$ oscillators.[1,22,23] In contrast, compound ***cis*-1a** also gives rise to two N–O stretching bands for terminal nitrosyls, but they appear at somewhat higher frequency and with reversed intensities. The N–O stretch for the bridging nitrosyl in these complexes is expectedly much less energetic, and the values recorded in KBr pellets were found to be substantially lower for ***cis*-1a** (1393 $cm^{-1}$) than for **1a** (1420 $cm^{-1}$), in agreement with the higher pyramidalization of the bridging nitrosyl at the *cis* isomer. The value recorded for the ditungsten complex **1b** was even lower (1360 $cm^{-1}$), but this lowering is likely due in part to the presence of heavier metal atoms in this molecule.

**DFT Studies on Trinitrosyl Complexes 1.** To gain more insight into the observed pyramidalization at the bridging NO ligand in compounds **1** and possible chemical effects derived thereof, and also to remove any influence of crystal packing forces on this structural distortion, we have carried out DFT calculations on all three compounds **1** in the gas phase (see Experimental Section and the SI for details). The optimized structures of **1b** and ***cis*-1a** are shown in Figure 2, and a selection of structural parameters for all three molecules is collected in Table 3

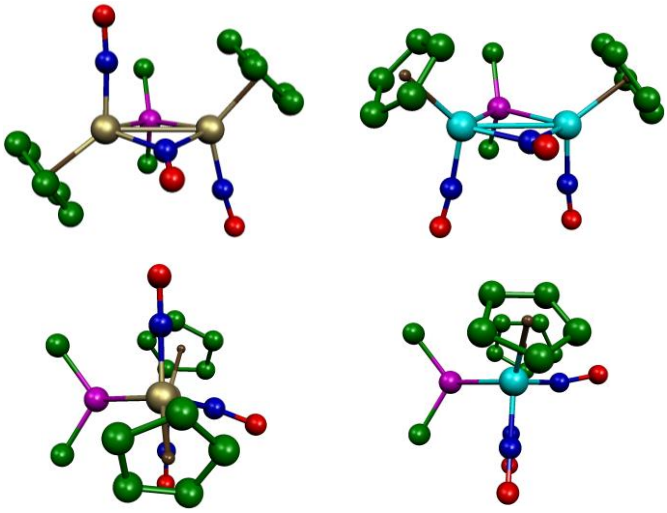

**Figure 2**. B3LYP-DFT-optimized structures of compounds **1b** (left) and ***cis*-1a** (right), with H atoms and Cy groups (except their $C^1$ atoms) omitted. Below, the corresponding projections along the Mo–Mo bonds are shown.

**Table 3.** B3LYP-DFT-computed Bond Lengths (Å) and Angles (°) for Compounds **1**[a]

| parameter | **1a**[b] | ***cis*-1a** | **1b** |
|---|---|---|---|
| M1–M2 | 2.922 | 2.954 | 2.909 |
| M1–P1 | 2.446 | 2.456 | 2.443 |
| M2–P1 | 2.456 | 2.454 | 2.454 |
| M1–N3 | 2.039 | 2.043 | 2.027 |
| M2–N3 | 2.038 | 2.041 | 2.025 |
| N3–O3 | 1.213 | 1.216 | 1.228 |
| M1–M2–N2 | 90.1 | 96.7 | 89.8 |
| M2–M1–N1 | 103.7 | 96.7 | 104.9 |
| $\Sigma$(N3) | 359.3 | 357.6 | 358.7 |
| $\alpha(pd)$ | 173.2 (0.12) | 167.8 (0.22) | 171.5 (0.16) |
| $\beta$ | 167.2 | 179.1 | 165.4 |
| $\nu$(N3–O3)/cm$^{-1}$ | 1594 | 1579 | 1529 |

[a] Labeling scheme and parameters as defined for Table 2. [b] Data taken from reference 11.

First we note that the optimized structures are generally in good agreement with the structures determined in the solid state, and confirm in all cases the presence of a pyramidalized bridging nitrosyl, although all computed distances involving the metal atoms are somewhat overestimated, as commonly found in these types of calculations,[24] and the experimental differences between these three molecules are not perfectly reproduced by calculation. The relative pyramidalization degrees are correctly predicted, they increasing in the sequence **1a** (0.12) < **1b** (0.16) < ***cis*-1a** (0.22), although the absolute *pd* values are lower than the figures derived from the diffraction data. In any case these results prove that (a) the observed nitrosyl pyramidalization is a genuine intramolecular effect, and not due to crystal packing forces, (b) it must have an electronic (rather than steric) origin, since it increases when replacing Mo with W atoms, and (c) is not related to the folding of the central M–P–M–N skeleton, since the latter increases in the series ***cis*-1a** << **1a** < **1b**. In agreement with all of this, we also

recall that a structure for **1a** with a bridging nitrosyl forced into a planar environment around the N atom (**1F**) was computed to be some 12 kJ/mol less stable than the actual structure of **1a**.[11] We finally note that the computed Gibbs free energy for ***cis*-1a** was some 15 kJ/mol higher than that of its transoid isomer **1a**, in agreement with the observed thermal rearrangement of ***cis*-1a** into **1a** in refluxing toluene solution.

In the case of **1a**, our earlier analysis of the atomic charges indicated that the actual structure of **1a** had a slightly more negative charge at the bridging N atom than the forced structure **1F**, suggesting that there might be a relationship between the pyramidalization of the bridging nitrosyl and accumulation of negative charge at the corresponding N atom. A similar analysis on the three trinitrosyls **1** produces Mulliken charges increasing in the order **1a** (–0.242 *e*) < ***cis*-1a** (–0.248 *e*) < **1b** (–0.306 *e*), so we conclude that the mentioned relationship might be valid for similar structures (ie. the transoid isomers **1a** and **1b**), but the overall stereochemistry of the molecule is an even more important factor, as the largest pyramidalization is observed for the cisoid isomer ***cis*-1a**. Incidentally, we note that these atomic charges are significantly higher than those computed for the terminal nitrosyls, and comparable to the negative charges computed for the O atoms of the bridging nitrosyls (–0.265 to –0.292 *e*). From this we conclude that, under conditions of charge control, electrophiles might be equally able to bind either the N or O atoms of the bridging nitrosyl ligand in these complexes.

Analysis of the frontier molecular orbitals computed for compounds **1** renders a similar picture in all three cases (see the SI): (a) a relatively low HOMO–LUMO gap of 2.83-2.91 eV (cf. 2.92 eV computed for the unsaturated complex $[W_2Cp_2(\mu\text{-}H)(\mu\text{-}PPh_2)(NO)_2]$ at the same level),[25] in agreement with the deep blue color of these compounds, (b) a LUMO being largely located at the bridging nitrosyl, with $\pi^*$(N–O) antibonding character, and (c) a metal–metal bonding orbital being the HOMO or very close to it. The antibonding nature of the LUMO is of interest, since population of this empty orbital would expectedly lead to a weakening of the N–O bond in the bridging nitrosyl ligand. This might be achieved upon reaction of complexes **1** with suitable bases or reducing reagents, in agreement with their experimental chemical behavior, to be discussed in the next sections.

**Oxidation Reactions of Complexes 1.** To examine the basic redox chemistry of compounds **1** we first tested their oxidation reactions, and found that all of them react rapidly with a mild oxidant as $[FeCp_2](BF_4)$ in dichloromethane solution at room temperature. To our surprise, the stoichiometric reaction of **1a** with this reagent yielded quantitatively the nitroxyl-bridged complex $[Mo_2Cp_2(\mu\text{-}PCy_2)(\mu\text{-}\kappa^1\text{:}\eta^2\text{-}HNO)(NO)_2](BF_4)$ (**3a**), a product rationally prepared in our preliminary study upon protonation of **1a** using $HBF_4{\cdot}OEt_2$ (see below).[11] In a similar way, the ditungsten

complex **1b** also reacts with $[FeCp_2](BF_4)$ to give the related nitroxyl-bridged derivative $[W_2Cp_2(\mu\text{-}PCy_2)(\mu\text{-}\kappa^1\text{:}\eta^2\text{-}HNO)(NO)_2](BF_4)$ (**3b**) in high yield (Scheme 2).

The unexpected formation of compounds **3a,b** can be rationalized by assuming that the reaction of compounds **1a,b** with the ferricenium cation first yields an unstable radical $[M_2Cp_2(\mu\text{-}PCy_2)(\mu\text{-}NO)(NO)_2]^+$ which rapidly would undergo H-atom abstraction, either from the solvent or from traces of water therein present. To check this hypothesis we carried out a cyclic voltammetry (CV) study of **1a** in dichloromethane solution (see the Experimental Section for details) and found that indeed **1a** undergoes a quasi-reversible oxidation at a potential close to that of the $FeCp_2^+/FeCp_2$ couple (+0.47 V, see Figure 3). This is followed by a second oxidation process at +0.96 V which is irreversible, but clearly not accessible in a preparative reaction using the ferricenium cation (incidentally, this second oxidation produces a new species on the electrode surface, as shown by the appearance of a new reduction wave at ca. –0.5 V in the corresponding CV diagram). A quasi-reversible reduction at −1.11 V is also clearly detected for **1a**, which therefore is expected to react with mild reducing reagents, a matter to be discussed later on.

**Scheme 2. Oxidation Reactions of Complexes 1**

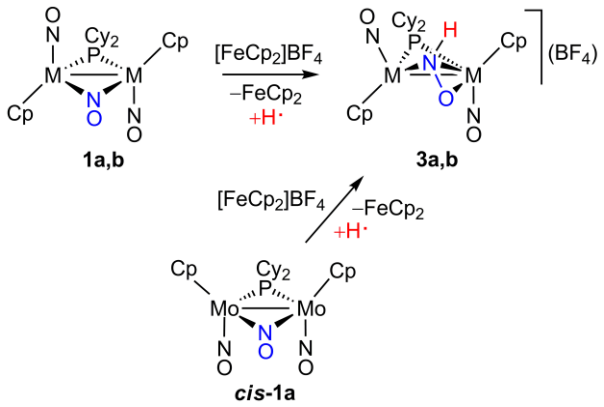


The reversibility of the first oxidation process detected for **1a** means that the corresponding radical **1a**$^+$ should be moderately stable, at least under conditions close to the CV experiments. Indeed, in a separate experiment we found that the reaction of **1a** with $[FeCp_2](BF_4)$, when carried out in a dichloromethane solution being also 0.1 M in $[NBu_4](PF_6)$ (same conditions as in the CV experiment), first gives a $^{31}P\{^1H\}$ NMR-silent solution (suggestive of the presence of a paramagnetic species) displaying a broad N–O stretch at 1645 $cm^{-1}$, which we identify as arising from the expected radical $[Mo_2Cp_2(\mu\text{-}PCy_2)(\mu\text{-}NO)(NO)_2]^+$ (**1a**$^+$) resulting from the one-electron oxidation of **1a**. This solution progressively transforms into one of the nitroxyl derivative **3a**, identified by a more energetic N–O stretch of the terminal nitrosyls at 1662 $cm^{-1}$ and a sharp $^{31}P$ NMR resonance (Table 1).

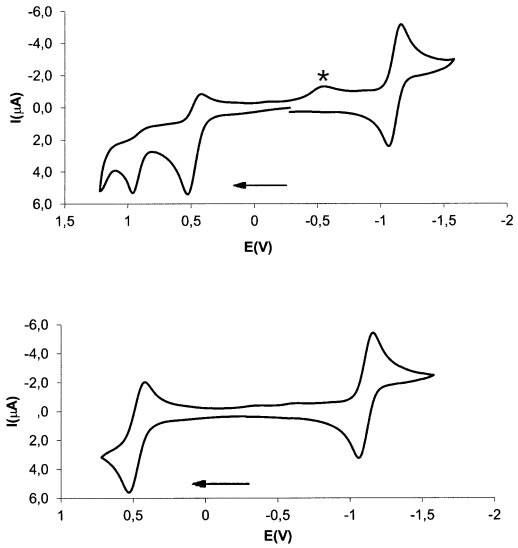


**Figure 3.** CV diagram of compound **1a** in $CH_2Cl_2$, at a scan rate of 100 $mVs^{-1}$, recorded from –1.6 V to +1.2 V (upper) and from –1.6 V to +0.7 V (lower). The peak marked with an asterisk is related to the irreversible second oxidation of the complex.

Isomer ***cis*-1a** also is readily oxidized by $[FeCp_2](BF_4)$ in dichloromethane solution at room temperature. However, this reaction yields quantitatively compound **3a**, it meaning that a fast *cis* to *trans* rearrangement takes place at some stage of this reaction. Moreover, we have found that this rearrangement can be of a catalytic nature, since a separated reaction between ***cis*-1a** and ca. 0.2 equiv of $[FeCp_2](BF_4)$ yielded neutral **1a** as the major product, along with smaller amounts of **3a**. We can rationalize all these observations by assuming the operation of an electron-transfer catalyzed isomerization mechanism, which is well precedented for organometallic compounds.[26] It is likely that removal of one electron from ***cis*-1a** would first give a radical ***cis*-1a$^+$** retaining the geometry of the neutral precursor (*step 1*, initiation). This radical, of high energetic content, would rapidly rearrange into a more stable isomer with a transoid arrangement of its MoCp(NO) fragments (**1a$^+$**, *step 2*). This would be equivalent to the (slow) *cis* to *trans* isomerization observed for neutral ***cis*-1a** upon thermal activation, here taking place rapidly at room temperature. The radical **1a$^+$** then might oxidize any remaining neutral ***cis*-1a**, thus yielding neutral **1a** and a new molecule of radical ***cis*-1a$^+$** (*step 3*), which then goes again through the sequence 2-3 until all neutral ***cis*-1a** is consumed, thus accomplishing a catalytic *cis* to *trans* isomerization of ***cis*-1a** very fast at room temperature.

***cis*-1a** + $FeCp_2^+$ → ***cis*-1a$^+$** + $FeCp_2$ (*step 1*)

***cis*-1a$^+$** → **1a$^+$** (*step 2*)

**1a$^+$** + ***cis*-1a** → **1a** + ***cis*-1a$^+$** (*step 3*)

***cis*-1a** → **1a** (*2 + 3*)

**Structure of Nitroxyl Complexes 3.** The structure of the dimolybdenum complex **3a** was reported in our preliminary study on the chemistry of **1a**.[11] It can be described as closely related to that of its parent compound, with the terminal nitrosyls also departing from an ideal antiparallel arrangement (Mo–Mo–NO angles ca. 90 and 108°), and the bridging nitrosyl now converted into a four-electron donor nitroxyl ligand due to the attachment of the added hydrogen to the N atom (Figure 4). In the crystal lattice, this H atom is involved in hydrogen bonding with the $BF_4^-$ counterion (NH···$FBF_3$ ca. 1.92 Å), which is not unexpected. The nitroxyl ligand is coordinated to the dimetal center in an alkenyl-like $\kappa^1:\eta^2$ fashion, with the N atom $\sigma$-bound to one metal atom *via* its lone electron pair (N3–Mo1 = 2.007(4) Å) and $\pi$-bound to the other metal atom *via* its double N–O bond (Mo2–N3 = 2.193(5), Mo2–O3= 2.092(4) Å). As a result of the latter interaction, this bond is significantly weakened, as judged from the N–O length of 1.348(6) Å, substantially longer than the distances of 1.19-1.24 Å measured in the few mononuclear complexes characterized so far with a nitroxyl ligand *N*-bound to a single metal centre.[27] A further, if indirect, indication of the strength of the $\eta^2$-interaction of the HNO ligand in **3a** can be found in the asymmetric coordination of the $PCy_2$ ligand, which is ca. 0.08 Å closer to the Mo1 atom. Overall, **3a** can be classified as a 34-electron complex, for which a Mo–Mo single bond has to be proposed, in agreement with the intermetallic separation of 2.9995(5) Å which, however, is ca. 0.1 Å longer than the corresponding distance in the parent compound **1a**.

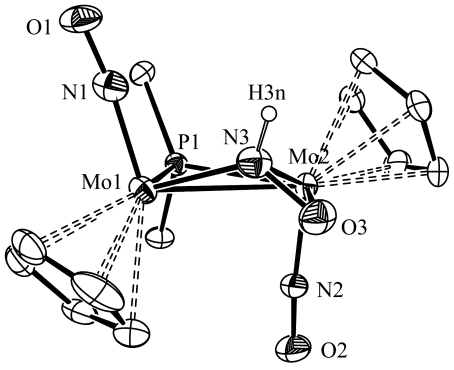


**Figure 4**. ORTEP diagram (30% probability) of compound **3a**, with most H atoms and Cy groups (except their $C^1$ atoms) omitted for clarity.[11] Selected bond lengths (Å) and angles (°): Mo1–Mo2 = 2.9995(5); Mo1–P1= 2.423(1); Mo2–P1 = 2.503(1); Mo1–N3 = 2.007(4); Mo2–N3 = 2.193(5); Mo2–O3= 2.092(4); N3–O3 = 1.348(6). Mo1–Mo2–N2 = 89.7(2); Mo2–Mo1–N1 = 108.0(1).

We should note that compound **3a** seems to be the first complex structurally characterized with a bridging nitroxyl ligand of any kind. Complexes bearing the related RNO ligands (R = alkyl, aryl) bridging two metal atoms, however, are not uncommon, although most of them display a $\mu$-$\kappa^1:\kappa^1$ coordination mode, rather than the $\mu$-$\kappa^1:\eta^2$ mode found in **3a** (Chart 3), with both modes formally providing the dimetal center with the same number (4) of electrons. In fact, only a few binuclear RNO-bridged complexes of the second type have been structurally characterized, of which none of them were

metal–metal bonded species.[28] Yet, all of them expectedly display quite elongated N–O separations, in the range 1.37-1.43 Å, as found for **3a**. We also note that a few complexes have been structurally characterized with RNO ligands in the $\mu$-$\eta^2$:$\eta^2$ coordination mode (Chart 3).

**Chart 3. Coordination Modes of Bridging RNO Ligands**

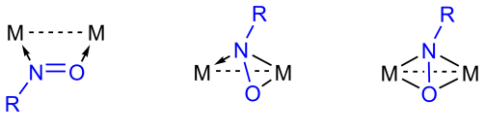


Spectroscopic data in solution for compounds **3a** and **3b** (Table 1 and Experimental Section) are similar to each other and consistent with the structure found in the solid state for **3a**. The terminal nitrosyl ligands give rise to two N–O stretches with the characteristic pattern of transoid $M_2(NO)_2$ oscillators, but some 70 $cm^{-1}$ higher in frequency than the neutral precursors, as expected for cationic species, while the presence of a N-bound H atom is denoted by the observation of highly deshielded $^1H$ NMR resonances at 12.2 and 11.0 ppm respectively, and a N–H stretch at 3304 $cm^{-1}$ in the case of **3a**. The asymmetric coordination of the nitroxyl ligand in these complexes is also consistent with the observation of quite different couplings of the P atom in **3b** with the inequivalent metal centers ($J_{PW}$ = 312 and 222 Hz), an effect which can be attributed in part to the different coordination numbers of the W atoms in the cation.[16]

**Protonation Reactions of Compound 1a.** The nitroxyl complexes **3** might be viewed as resulting from protonation of the corresponding trinitrosyl precursors **1**. Indeed the reaction of the dimolybdenum complex **1a** with $HBF_4{\cdot}OEt_2$ gives the corresponding nitroxyl derivative **3a**, identical to the product obtained in the oxidation reactions discussed above. This result, however, is somewhat surprising since, although both the N and O atoms of the bridging nitrosyl in **1a** bear comparable atomic charges as noted above, and are therefore suitable for direct attachment of a hard electrophile as the proton, the O atom of the bridging nitrosyl is more exposed for external attack, therefore more favored as a protonation site on steric grounds. In addition, a proton attack at the O atom should cause a smaller structural rearrangement in the molecule, then being favored also on kinetic grounds.[29] Finally, protonation at the O site in **1a** should lead to a hydroximido ligand, a process previously observed at different nitrosyl-bridged clusters (usually to give $\mu_3$-NOH ligands), and even at some binuclear complexes.[30]

In order to examine the viability of *O*-protonation derivatives of **1a** we carried out DFT calculations on the putative hydroximido-bridged cation $[Mo_2Cp_2(\mu\text{-}PCy_2)(\mu\text{-}NOH)(NO)_2]^+$ (**3a'**) potentially following from *O*-protonation at the bridging nitrosyl of **1a**. We have found that such a complex is a genuine minimum in the corresponding

potential energy surface, and expectedly has a structure little disturbed with respect to the parent **1a**, with relatively short Mo–Mo and Mo–N lengths (2.983 and ca. 1.98 Å) (Figure 5). However, the computed Gibbs free energy for this cation is some 48 kJ/mol higher than the value computed for the nitroxyl isomer **3a** at the same level. Therefore we conclude that, even if an hydroximido tautomer might be formed first upon proton attack at the bridging nitrosyl of **1a**, a fast rearrangement of the latter into its more stable nitroxyl isomer likely would take place rapidly, either in an intermolecular or intramolecular fashion. To gain complementary information on this matter, we then analyzed the methylation reactions of compounds **1a,b**.

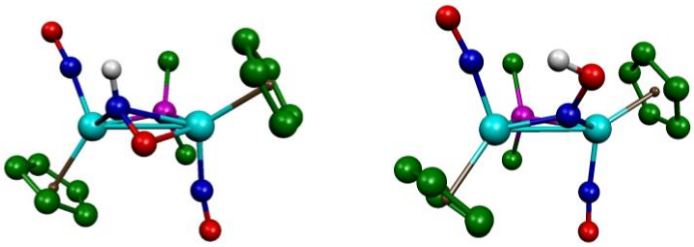

**Figure 5**. B3LYP-DFT-optimized structures of the cation in the nitroxyl complex **3a** (left) and its hydroximido isomer **3a'** (right), with most H atoms and Cy groups (except their $C^1$ atoms) omitted, and labeling as in Figure 4. Relative Gibbs free energies were 0 and, +48 kJ/mol, respectively. Selected bond lengths (Å) for **3a**: Mo1–Mo2 = 3.072; Mo1–N3 = 2.032; Mo2–N3 = 2.226; Mo2–O3 = 2.095; N3–O3 = 1.348. Isomer **3a'**: Mo1–Mo2 = 2.983; Mo1–N3 = 1.979; Mo2–N3 = 1.992; N3–O3 = 1.358.

**Methylation Reactions of Compounds 1.** Compounds **1a,b** are not nucleophilic enough to react at room temperature with a mild methylation reagent as MeI. Out of them, the ditungsten complex **1b** displays a higher nucleophilicity, because it reacts at room temperature with $CF_3SO_3Me$ within a few minutes, to give the corresponding nitrosomethane derivative $[W_2Cp_2(\mu\text{-}PCy_2)(\mu\text{-}\kappa^1\text{:}\eta^2\text{-}MeNO)(NO)_2](CF_3SO_3)$ (**4b**), whereas the same reaction of **1a** was very slow under the same conditions (Scheme 3). Methylation of the dimolybdenum complex **1a** could be more conveniently accomplished using a stronger reagent as $[Me_3O]BF_4$, the reaction then being completed in a few minutes at room temperature to give the nitrosomethane derivative $[Mo_2Cp_2(\mu\text{-}PCy_2)(\mu\text{-}\kappa^1\text{:}\eta^2\text{-}MeNO)(NO)_2](BF_4)$ (**4a**). In both cases, significant amounts of the corresponding nitroxyl complexes **3a,b** were formed, likely due to hydrolysis of the methylation reagents during reaction. Besides this, the nitrosomethane complexes were obtained in both cases as a mixture of two isomers (**A** and **B** in Chart 4) with the **A**/**B** ratio being ca. 3/1 in both cases. Attempts to purify the ditungsten complex **4b** were unsuccessful. Fortunately, the dimolybdenum complex could be conveniently purified in a conventional way after anion exchange with $Na[BAr'_4]$ in dichloromethane solution (Ar´ = 3,5-$C_6H_3(CF_3)_2$). This yielded the salt $[Mo_2Cp_2(\mu\text{-}PCy_2)(\mu\text{-}\kappa^1\text{:}\eta^2\text{-}MeNO)(NO)_2](BAr'_4)$ (**4a**) which, after chromatographic workup, was isolated as a ca. 2/1 mixture of corresponding isomers **A** and **B**. Separate experiments revealed that these

isomers were not in equilibrium, but just were too difficult to be properly separated from each other by chromatography.

**Scheme 3. Methylation of Complexes 1a,b**[a,b]

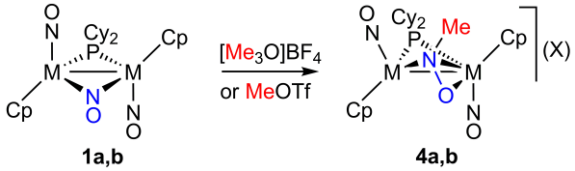


[a] X = $BF_4$, $CF_3SO_3$. Complex **4a** was eventually isolated as the $[B\{3,5\text{-}C_6H_3(CF_3)_2\}_4]^-$ salt (see text). [b] In both reactions, significant amounts of the corresponding nitroxyl complexes **3a,b** were formed (see text).

Spectroscopic data in solution for compounds **4a,b** (Table 1 and Experimental section) were comparable to those of the corresponding nitroxyl complexes **3a,b** irrespective of the isomer under consideration (**A** or **B**), except for the NMR resonances derived from the N–H group in the nitroxyl complexes, here replaced by resonances characteristic of N–Me groups ($\delta_H$ ca. 4 ppm, $\delta_C$ ca. 70 ppm). We propose that isomers **A** and **B** display the same $\mu$-$\kappa^1$:$\eta^2$ coordination mode of the nitrosomethane ligand, with the major isomer **A** corresponding to the structure found in the solid state for the nitroxyl complex **3a**, and isomer **B** being obtained by just exchanging $\kappa^1$ and $\eta^2$ bindings of the bridging ligand between metal atoms (Chart 4). We note that this is an isomerism previously found in alkenyl-bridged complexes of type $[M_2Cp_2(\mu\text{-}PCy_2)(\mu\text{-}\kappa^1\text{:}\eta^2\text{-}CR{=}CH_2)(NO)_2]$ (M= Mo, W),[31] which are structurally related to complexes **4**.

**Chart 4. Solution Conformers for Complexes 4**

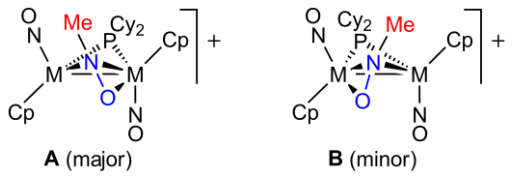


To support the above hypothesis we carried out DFT calculations on the cation of compound **4a**, and found that isomer **A** actually is more stable than **B** by 15 kJ/mol (Figure 6). The higher energy of **B** likely is due to a slightly worse steric fitting of the nitrosomethane ligand at the dimetal center in this isomer, as concluded from the observation of somewhat higher Mo–Mo and average Mo–N3 lengths for **B** (by ca. 0.05 and 0.08 Å, respectively). We also checked the structure of a putative methoxymido-bridged isomer $[Mo_2Cp_2(\mu\text{-}PCy_2)(\mu\text{-}NOMe)(NO)_2]^+$ (**4a'**), and found it to be 58 kJ/mol less stable than **A**, thus paralleling the findings concerning the nitroxyl complex **3a** discussed above.

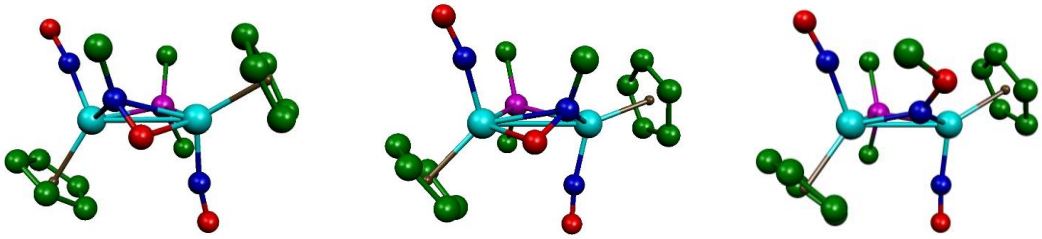

**Figure 6**. B3LYP-DFT-optimized structures of two conformers of the nitrosomethane complex cation of compound **4a** (**A**, left and **B**, middle) and its methoximido isomer **4a'** (right), with H atoms and Cy groups (except their $C^1$ atoms) omitted, and labeling as in Figure 4. Relative Gibbs free energies were 0, +15 and +58 kJ/mol, respectively. Selected bond lengths (Å) for conformer **A**: Mo1–Mo2 = 3.054; Mo1–N3 = 2.045; Mo2–N3 = 2.276; Mo2–O3 = 2.096; N3–O3 = 1.347. Conformer **B**: Mo1–Mo2 = 3.108; Mo1–N3 = 2.381; Mo2–N3 = 2.021; Mo1–O3 = 2.088; N3–O3 = 1.336. Isomer **4a'**: Mo1–Mo2 = 2.970; Mo1–N3 = 2.008; Mo2–N3 = 1.989; N3–O3 = 1.342.

**Reduction Reactions of Complexes 1.** All three compounds **1** reacted readily with Na(Hg) in tetrahydrofuran solution to give in moderate yield the corresponding amido-bridged derivatives with retention of the stereochemistry, so that the transoid isomers **1a,b** gave the transoid complexes $[M_2Cp_2(\mu\text{-}PCy_2)(\mu\text{-}NH_2)(NO)_2]$ (**5a,b**), while ***cis*-1a** rendered selectively the cisoid isomer *cis*-$[Mo_2Cp_2(\mu\text{-}PCy_2)(\mu\text{-}NH_2)(NO)_2]$ (***cis*-5a**) (Scheme 4). The overall process requires a hydrogen source, very likely trace water molecules present in the solvent, and can be represented by the overall equation 2.

$$M_2(\mu\text{-}NO) + 4e^- + 3H_2O \rightarrow M_2(\mu\text{-}NH_2) + 4OH^- \qquad \text{(eq. 2)}$$

We have examined in more detail the reduction reactions of the dimolybdenum complex **1a**, and found that a milder reducing reagent as Zn(Hg) also accomplishes the same transformation, which suggests that the one-electron reduction observed at ca. –1.1 V in the CV experiment discussed above likely is responsible for the initiation of the multistep procedure required to reach the amido complex eventually isolated, although no intermediate species could be detected when monitoring the relatively slow formation of **5a** when using zinc amalgam. Moreover, the addition of a small amount of water to the solvent improved significantly the amount of **5a** being formed, which could be isolated in ca. 65% yield after workup, in agreement with eq. 2. Interestingly, we found that **5a** was formed slowly as the unique organometallic product upon reaction of **1a** with CO (40 atm) in toluene at 353 K, thus suggesting that quite mild reducing agents might be able to trigger an N–O cleavage at the bridging nitrosyl of this complex. Even some **5a** is formed in the thermal reactions of **1a** with phosphites, a matter to be discussed below, along with possible pathways to accomplish the $M_2(\mu\text{-}NO)$ to $M_2(\mu\text{-}NH_2)$ transformation. Surprisingly, $H_2$ failed to react with **1a** even under forcing conditions (30 atm, toluene, 353 K). We finally should note that related transformations of bridging nitrosyls have been described previously (eg. $[Cr_2Cp_2(\mu\text{-}NO)_2(NO)_2]$ into $[Cr_2Cp_2(\mu\text{-}NO)(\mu\text{-}NH_2)(NO)_2]$ or $[Cr_2Cp_2(\mu\text{-}NH_2)_2(NO)_2]$), although

this typically required strong hydride donors or an hydrogenation catalyst, and were of poor selectivity.[7]

**Scheme 4. Reduction Reactions of Complexes 1**

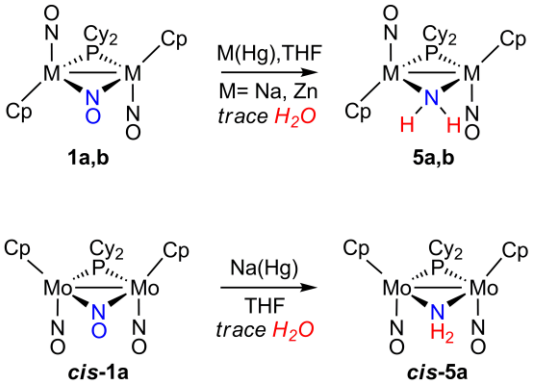


**Structural Characterization of Amidocomplexes 5.** The structure of the dimolybdenum complex **5a** was determined in our preliminary study on this chemistry (Figure 7).[11] The molecule can be derived from that of the parent compound **1a** by just replacing the bridging nitrosyl ligand with an isoelectronic $NH_2$ group, but this has some significant structural effects: (a) the central M–P–M–N skeleton becomes almost flat (P–Mo–Mo–N = 177.3°), and the terminal nitrosyls become almost perfectly antiparallel (Mo–Mo–N angles ca. 98°), and (b) the intermetallic length is slightly shortened by ca. 0.03 Å while the bridging amido ligand displays Mo–N lengths ca. 0.1 Å longer than the bridging nitrosyl of **1a**, this suggesting a weaker binding of the $NH_2$ group. Yet, these Mo–N lengths are comparable to the values of ca. 2.15 Å measured in $[Mo_2Cp_2(\mu\text{-}NH_2)(\mu\text{-}SMe)_3]$, which seems to be the only other organometallic $Mo_2$ amido complex structurally characterized to date.[32]

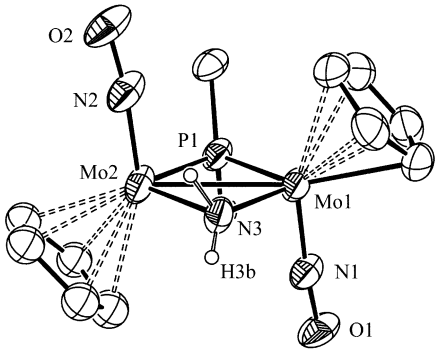


**Figure 7**. ORTEP diagram (30% probability) of compound **5a** with most H atoms and Cy groups (except their $C^1$ atoms) omitted.[11] Selected bond lengths (Å) and angles (°): Mo1–Mo2 = 2.8654(8); Mo1–P1 = 2.396(2); Mo1–N1 = 1.760(7); Mo1–N3 = 2.126(8); Mo2–P1 = 2.395(2); Mo2–N3 = 2.126(7); Mo–N2 = 1.753(9). Mo1–Mo2–N2 = 97.9(2); Mo2–Mo1–N1 = 97.2(2).

The IR and $^{31}P\{^1H\}$ NMR spectra for **5a,b** in solution (Table 1) are comparable to those of the parent complexes **1a,b**, but the N–O stretches of the terminal nitrosyls are significantly less energetic by some 30 $cm^{-1}$, which is indicative of the dominant donor

properties (minimum acceptor character) of the bridging amido ligand, when compared to NO. The equivalent H atoms of the $NH_2$ ligand expectedly give rise to a single $^1H$ NMR resonance, located at ca. 3.5 ppm, and to two N–H stretches in the IR spectrum, located at 3382 and 3325 $cm^{-1}$ in the case of **5a**. Interestingly, the observed P–W coupling of 363 Hz for **5b** approaches the value of ca. 360 Hz expected on the basis of the correlation found for a family of complexes of general formula *trans*-[$W_2Cp_2(\mu$-$PPh_2)(\mu$-X)$(NO)_2$], where X is a 3-electron donor ligand,[33] after allowing for the ca. 20 Hz lower figures usually found when comparing W–$PCy_2$ and W–$PPh_2$ couplings. In contrast, the P–W coupling in the parent compound **1b** is only 340 Hz, a reduction possibly related to the pyramidalization of the bridging NO ligand in this molecule.

The structural differences of isomer ***cis*-5a** are readily apparent from the IR and $^1H$ NMR spectra. In the first case, two N–O stretches are found at frequencies only slightly higher than those of **5a**, but their relative intensity is reversed, while the amido H atoms are no longer equivalent, then giving rise to separate NMR resonances at 3.84 and 3.21 ppm. Other spectroscopic features are as expected and deserve no further comments.

**Reactions of Complex 1a with Phosphites.** As indicated above, compound **1a** was found to slowly render the amido complex **5a** through reaction with CO under forcing conditions. This suggested the viability for **1a** of a N–O cleavage reaction path requiring just a good O-atom acceptor, rather than an electron-releasing species. In the CO reaction, the added reagent would be likely eliminated as $CO_2$. To further explore this sort of O-atom abstraction processes we then examined the reactions of the dimolybdenum complex **1a** with different P-donors such as phosphines and phosphites. Surprisingly, phosphines such as $PPh_3$ and even the very basic $PMe_3$ failed to react with **1a** even when using a large excess of reagent in refluxing toluene solution. Phosphites such as $P(OEt)_3$ and $P(OPh)_3$, however, reacted slowly under the same conditions to give the corresponding phosphoraniminato-bridged derivatives [$Mo_2Cp_2(\mu$-$PCy_2)\{\mu$-$NP(OR)_3\}(NO)_2$] (R = Et (**6**), Ph (**7**)) as major products (Scheme 5), the reaction being faster for the aryl phosphite (completion times 20 and 6 h, respectively). The reaction with $P(OPh)_3$ also yielded variable, but smaller amounts of the amido complex **5a**, likely due to the presence a trace water in the reaction medium. Separate experiments indicated that water itself did not react with **1a** in refluxing toluene after 6 h; however, on purpose addition of water to the solvent caused the reaction between **1a** and excess $P(OPh)_3$ in refluxing toluene to give the amido complex **5a** as major product, although the formation of **7** was not fully suppressed. All these experiments prove that the N–O cleavage of **1a** is actually triggered by reaction with the added phosphite, although the products eventually isolated depend on the presence of different species in solution, a matter to be discussed below. The O atom of the bridging nitrosyl ligand is removed as the corresponding phosphate $P(O)(OR)_3$, which was identified in all these reaction

mixtures through its characteristic $^{31}$P NMR resonance. We should finally note that, although related transformations have long been known for mononuclear nitrosyl complexes,[1a] the N–O bond cleavage of a bridging nitrosyl ligand by a P-donor ligand has not been previously reported. Moreover, complexes **6** and **7** seem to be the first isolated complexes with a $X_3P{=}N^-$ ligand bearing alkoxy substituents. Recently, a mononuclear iron(IV) nitride complex was reported to react with phosphites to give the corresponding phosphoraniminato derivatives, although these products were not actually isolated.[34]

**Scheme 5. Reactions of Compounds 1a with Phosphites**

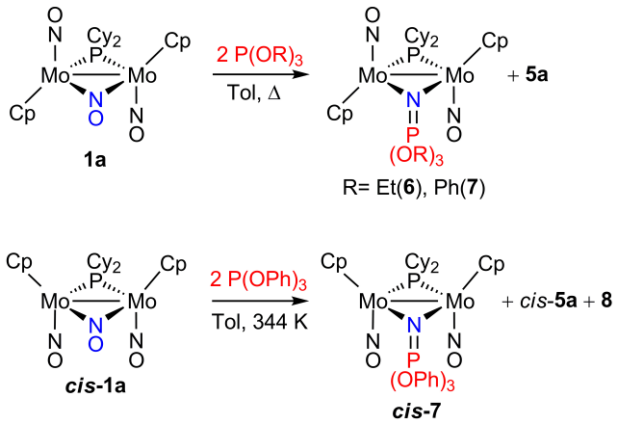


**Structure of the Phosphoraniminato-Bridged Complexes 6 and 7.** The structure of the $P(OPh)_3$ derivative **7** was determined during our preliminary study on the chemistry of **1a** (Figure 8).[11] The molecule can be derived from that of the parent compound **1a** by just replacing the oxygen atom of the bridging nitrosyl ligand with a phosphite molecule, whereby a new *N*:*N*-bound phosphoraniminato ligand is formed. The coordination sphere around the metal centers is similar to the one observed for the amido-bridged complex **5a**, this including an almost flat central Mo–P–Mo–N skeleton (folding angle ca. 175º), almost antiparallel terminal nitrosyls (M–M–NO angles ca. 96 and 102º), Mo–N(bridging) lengths of ca. 2.12 Å, and an intermetallic separation of ca. 2.88 Å. We should remark that **7** is the first structurally characterized complex with a $X_3P{=}N^-$ ligand bearing alkoxy substituents. The quite short P–N length of 1.515(3) Å in **7** can be viewed as indicative of a very strong double bond, it actually being shorter than the reference P–N double-bond length of 1.57 Å,[35] and in any case shorter than the values of 1.54-1.65 Å measured in all previous complexes having $\mu$-N=$PX_3$ ligands bearing alkyl, aryl or even $NR_2$ substituentes.[36]

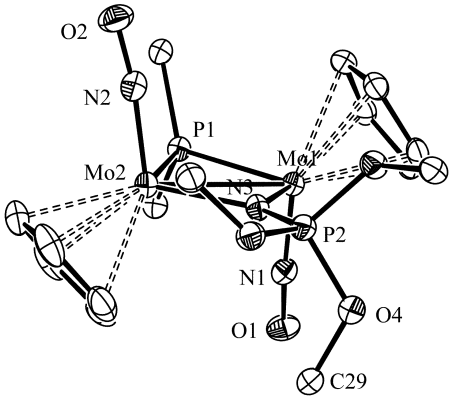


**Figure 8.** ORTEP diagram (30% probability) of compound **7**, with H atoms, Cy groups, and Ph rings (except their $C^1$ atoms) omitted for clarity.[11] Selected bond lengths (Å) and angles (°): Mo1–Mo2 = 2.8778(4); Mo1–P1 = 2.388(1); Mo1–N1 = 1.766(4); Mo1–N3 = 2.131(3); Mo2–P1 = 2.396(1); Mo2–N2 = 1.769(4); Mo2–N3 = 2.104(3); N3–P2 = 1.515(3). Mo2–Mo1–N1 = 96.0(1); Mo1–Mo2–N2 = 101.9(1).

Spectroscopic data in solution for **6** and **7** (Table 1 and Experimental Section) also are comparable to those of the amido complex **5a**, except for the presence of a second, quite shielded resonance in the $^{31}P\{^1H\}$ NMR spectrum corresponding to the phosphoraniminate ligand, located at 26.9 (**6**) and 5.2 ppm (**7**). Noticeably, the N–O stretches of these complexes are some 10 and 20 $cm^{-1}$ lower than the corresponding stretches in **5a**, respectively, this being an indication of the extremely efficient donor-properties of the phosphoraniminate ligand in these complexes.

**Reactions of Complex *cis*-1a with P(OPh)$_3$.** To check the influence of the stereochemistry at the dimetal centre on the N–O cleavage reactions leading to complexes **6** and **7** we examined the reaction between isomer ***cis*-1a** and triphenyl phosphite in toluene solution. Fortunately, this isomer is more reactive than **1a**, so this reaction can be carried out well below the boiling point of the solvent, to avoid the thermal *cis* to *trans* rearrangement of the starting material. In this way, the reaction between ***cis*-1a** and a five-fold excess $P(OPh)_3$ is completed in 4 days at 344 K, to yield the corresponding phosphoraniminato complex *cis*-[$Mo_2Cp_2(\mu$-$PCy_2)\{\mu$-$NP(OPh)_3\}(NO)_2$] (***cis*-7**) as major product, along with smaller amounts of a second, uncharacterized complex (see the Experimental Section), and trace amounts of the amido complex ***cis*-5a**. The formation of ***cis*-7** and ***cis*-5a** in this reaction, with no presence of the corresponding transoid isomers, as revealed by inspection of the $^{31}P\{^1H\}$ NMR spectra of the crude reaction mixtures, indicates that the N–O bond cleavage process under study takes place with retention of the overall stereochemistry at the dimetal center.

As for compound ***cis*-7**, the retention of the cisoid conformation of the starting material ***cis*-1a** is clearly denoted by the pattern of the N–O stretches of the terminal nitrosyls, similar to that of ***cis*-5a**, although frequencies were some 12 $cm^{-1}$ lower, as

found for the transoid isomers (Table 1). Other spectroscopic data for ***cis*-7** are comparable to those of its transoid isomer **7** and deserve no particular comment.

**Scheme 6. Pathways in the Reactions of Compounds 1 with Phosphites**[a]

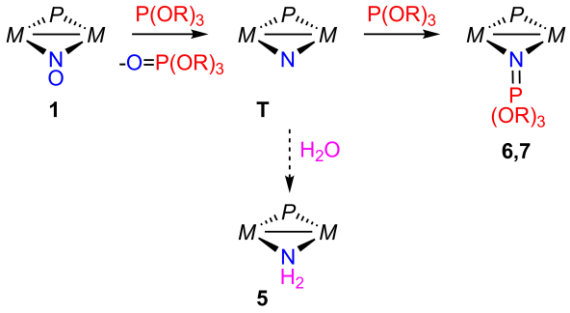


[a] *M* = MCp(NO), M = Mo, W; *P* = $PCy_2$.

**Pathways in the Reactions of Compounds 1 with Phosphites.** It has long been known that some mononuclear nitrosyl complexes undergo N–O cleavage reactions with phosphines to give the corresponding phosphine oxides, while the resulting nitride ligand is usually trapped as a phosphoraniminate, isocyanate or another ligand.[1a] Our data suggest that a similar reaction takes place on the bridging nitrosyl ligand of compounds **1** by the action of phosphites. By recalling that the LUMO of compounds **1** is mainly located at the bridging nitrosyl and has a $\pi^*$(N-O) antibonding character, it is then likely that an initial acid-base interaction of compounds **1** (acting as acceptor molecules) with a phosphite (acting as a donor) would result in a weakening of the N–O bond. Yet, the experimental observation that even a basic and small phosphine such as $PMe_3$ failed to react with **1a** suggests that the initial interaction between compounds **1** and a P-donor molecule is more complex, perhaps also involving a backbonding interaction from the dimetal site to the phosphite. In any case, this initial N–O bond cleavage reaction would yield a phosphate molecule (detected in the reaction mixture, as noted above) and an undetected nitrido-bridged intermediate **T** (Scheme 6). Binuclear complexes bearing an angular bridging nitride are extremely rare and expectedly quite reactive. Interestingly, Arikawa et al. have very recently reported the formation of a related but isolable nitride-bridged complex upon reduction of a nitrosyl-bridged $Ru_2$ complex in the presence of acid.[37] However, the expected evolution of a reactive molecule as intermediate **T** would be the coupling reaction with a second phosphite molecule to give the phosphoraniminato complexes **6** and **7** eventually isolated. Since the above elemental steps do not require direct coordination of phosphite to the metal atoms, then the overall reaction should occur with retention of the stereochemistry at the dimetal site, as observed. In the presence of water, however, intermediate **T** might undergo a competitive reaction with $H_2O$ molecules to eventually yield the amido complexes **5**, also with retention of the stereochemistry of the dimetal centre. This side transformation obviously requires several elemental steps and might also involve the

participation of additional phosphite molecules as oxygen scavengers, but the exact sequence of events is currently unknown. In the end, however, we trust that the nitride intermediates **T** resulting from the initial nitrosyl deoxygenation step would be eventually responsible for the formation of any phosphoraniminate or amide ligands formed in these reactions. Interestingly, similar results were reported recently for an azido-bridged dicobalt complex, thought to generate a transient nitrido-bridged complex reacting with $PMe_3$ or protons to give respectively the corresponding $N{=}PMe_3$- or $NH_2$-bridged derivatives,[38] although the elemental steps involved are not identical to those taking place at our dimolybdenum complexes.

## Concluding Remarks

Compounds **1** bear a bridging nitrosyl ligand displaying a significant pyramidalization at the N atom which is higher for W (instead of Mo) atoms and even higher for cisoid (instead of transoid) isomers. This geometrical departure from the expected trigonal planar environment is a genuinely intramolecular effect and seems to be electronic (instead of steric) in origin. The bridging nitrosyl ligand in these complexes bears comparable negative charges at the N and O atoms, which makes these sites suitable for attachment of hard acids, while the LUMO in all cases is largely centered in this ligand and has $\pi^*$(N–O) antibonding character, this leading to an expectation of N–O bond weakening upon reactions with Lewis bases or reducing reagents, confirmed by experiment. Complexes **1** appear to be protonated or methylated at the N site of the bridging nitrosyl to give the corresponding $\mu$-$\kappa^1$:$\eta^2$-bound nitroxyl or nitrosomethane complexes respectively, which are some 50 kJ/mol more stable that the corresponding hydroximido- or methoximido-bridged tautomers. Thus, an electrophilic attack at the O site followed by a fast tautomerization cannot be excluded in these reactions. The redox reactions of compounds **1** also involve the bridging nitrosyl ligand in all cases; removal of one electron from the transoid compounds **1a,b** gives first the corresponding radical cations $[M_2Cp_2(\mu\text{-}PCy_2)(\mu\text{-}NO)(NO)_2]^+$, which rapidly abstract a H atom from the solvent or traces of water to eventually yield the above nitroxyl complexes, while removal of one electron from ***cis*-1a** catalyses a fast *cis* to *trans* isomerization. Reduction of compounds **1** with electron releasing substances (Na(Hg), Zn(Hg)) or with O-atom acceptor molecules (CO, phosphites) in the presence of water, even in trace amounts, yields the corresponding amido-bridged derivatives with retention of stereochemistry, while phosphites yield the corresponding phosphoraniminato-bridged derivatives if no water is present. These results can be interpreted by assuming that CO and phosphites are able to abstract the O atom of the bridging nitrosyl to give a nitrido-bridged intermediate which then rapidly reacts with a second phosphite molecule or with water molecules, to yield the products eventually

isolated. All these N–O bond cleavage reactions are quite unusual for conventional bridging nitrosyls and might be related to the pyramidalization observed for this ligand in complexes **1**, although further studies will be needed to confirm or refute such hypothesis. In particular, it would be desirable to find new complexes bearing bridging NO ligands with a pyramidalization degree higher than the one observed for ***cis*-1a** (*pd* = 0.30), because the latter proved to be the most active species in the above deoxygenation reactions.

## Experimental Section

**General Procedures and Starting Materials.** All manipulations and reactions were carried out under an argon (99.995%) atmosphere using standard Schlenk techniques. Solvents were purified according to literature procedures, and distilled prior to use.[39] Complexes $[M_2Cp_2(\mu\text{-}H)(\mu\text{-}PCy_2)(CO)_4]$ (M = Mo, W),[14] **1a**,[11] **2a**,[11] **7**,[11] $[FeCp_2]BF_4$,[40] and $Na[B\{3,5\text{-}C_6H_3(CF_3)_2\}_4]$ ($NaBAr'_4$),[41] were prepared as described previously, and all other reagents were obtained from the usual commercial suppliers and used as received, unless otherwise stated. Petroleum ether refers to that fraction distilling in the range 338-343 K. Photochemical experiments were performed using Pyrex Schlenk tubes cooled by tap water (ca. 288 K). A 400 W medium-pressure mercury lamp placed ca. 1 cm away from the Schlenk tube was used for these experiments. Filtrations were carried out through diatomaceous earth unless otherwise stated. Chromatographic separations were carried out using jacketed columns refrigerated by tap water (ca. 288 K) or by a closed 2-propanol circuit kept at the desired temperature with a cryostat. Commercial aluminum oxide (activity I, 70-290 mesh) was degassed under vacuum prior to use. The latter was mixed under nitrogen with the appropriate amount of water to reach activity IV. IR stretching frequencies of CO, NO and NHR ligands were measured in solution (using $CaF_2$ windows), Nujol mulls, or KBr pellets, are referred to as $\nu$(XY) (X = C, N; Y = O, H) and are given in wave numbers ($cm^{-1}$). Nuclear magnetic resonance (NMR) spectra were routinely recorded at 300.13 ($^1H$), 121.50 ($^{31}P\{^1H\}$) and 75.46 ($^{13}C\{^1H\}$) MHz, at 298 K in $CD_2Cl_2$ solution unless otherwise stated. Chemical shifts ($\delta$) are given in ppm, relative to internal tetramethylsilane ($^1H$, $^{13}C$) or external 85% aqueous $H_3PO_4$ solutions ($^{31}P$). Coupling constants (*J*) are given in hertz. Electrochemical studies of **1a** were carried out using a conventional potentiostat in conjunction with a three-electrode cell under a nitrogen atmosphere. The auxiliary electrode was a platinum wire and the working electrode a platinum disc. The reference electrode was a silver wire. Solutions were 0.001 M in compound **1a** and 0.1 M in $[NBu_4](PF_6)$ as the supporting electrolyte in $CH_2Cl_2$. The potentials given are referenced to the one-electron oxidation of $[Fe(\eta^5\text{-}C_5H_5)_2]$, taken as 0.47 V.

**Preparation of [$W_2Cp_2(\mu$-$PCy_2)(\mu$-$NO)(NO)_2$] (1b)**. Solid $NaNO_2$ (0.140 g, 2.03 mmol) was added to a solution of compound **2b** (0.183 g, 0.204 mmol) in tetrahydrofuran (20 mL), and the mixture was stirred at 323 K for 80 min to give a greenish solution. The solvent was then removed under vacuum, the residue was extracted with dichloromethane/petroleum ether (1/10) and the extracts were filtered. Removal of solvents from the filtrate yielded compound **1b** as a blue solid (0.078 g, 49%) containing small amounts of $P(O)HCy_2$. This product can be further purified through chromatography on alumina at 253 K, but substantial decomposition occurs along the column. The crystals used in the X-ray diffraction study of **1b** were grown by the slow diffusion of a layer of petroleum ether into a concentrated dichloromethane solution of the complex at 253 K. Anal. Calcd for $C_{22}H_{32}N_3O_3PW_2$: C, 33.65; H, 4.11; N, 5.35. Found: C, 33.79; H, 4.14; N, 4.81. $^1$H NMR: $\delta$ 5.79 (s, 10H, Cp), 2.35-1.00 (m, 22H, Cy).

**Preparation of *cis*-[$Mo_2Cp_2(\mu$-$PCy_2)(\mu$-$NO)(NO)_2$] (*cis*-1a)**. A solution of compound **1a** (0.045 g, 0.074 mmol) in toluene (10 mL) was irradiated with visible-UV light at 288 K for 80 min to give a blue greenish solution. The solvent was then removed under vacuum, the residue was extracted with dichloromethane/petroleum ether (1/2) and the extracts were chromatographed on an alumina column at 288 K. Elution with dichloromethane/petroleum ether (1/1) gave a blue-greenish fraction yielding, after removal of solvents, compound ***cis*-1a** as a dark blue solid (0.032 g, 71%). The crystals used in the X-ray diffraction study of ***cis*-1a** were grown by the slow diffusion of layers of toluene and petroleum ether into a concentrated dichloromethane solution of the complex at 253 K. Anal. Calcd for $C_{22}H_{32}N_3O_3PMo_2$: C, 43.36; H, 5.29; N, 6.90. Found: C, 43.03; H, 5.06; N, 6.39. $^1$H NMR: $\delta$ 5.42 (s, 10H, Cp), 3.00 (m, 1H, Cy), 2.35-1.20 (m, 21H, Cy).

**Preparation of [$W_2Cp_2(\mu$-$PCy_2)(CO)_2(NO)_2$][$BF_4$] (2b)**. Solid $Na_2CO_3$ (0.125 g, 1.179 mmol) and [NO]($BF_4$) (0.130 g, 1.113 mmol) were added to a solution of complex [$W_2Cp_2(\mu$-H)($\mu$-$PCy_2)(CO)_4$] (0.300 g, 0.371 mmol) in dichloromethane (20 mL), and the mixture was stirred at room temperature for 2.5 h to give a brown-orange solution which was filtered. Removal of solvent from the filtrate under vacuum yielded compound **2b** as a brown solid (0.213 g, 64%). In solution, this compound displays two isomers (**A** and **B**), with an equilibrium **A**/**B** ratio of ca. 5/1 in $CD_2Cl_2$ at room temperature. Anal. Calcd for $C_{24}H_{32}BF_4N_2O_4PW_2$: C, 32.10; H, 3.59; N, 3.12. Found: C, 31.82; H, 3.65; N, 2.81. $\nu$(CO) ($CH_2Cl_2$): 2017 (s), 1981 (w, sh); $\nu$(NO) ($CH_2Cl_2$): 1665 (vs). $\nu$(CO) (THF): 2012 (s), 1980 (m); $\nu$(NO) (THF): 1681 (vs), 1657 (s). *Data for Isomer **A***: $^1$H NMR: $\delta$ 6.06 (s, 10H, Cp), 3.10-0.20 (m, 22H, Cy). *Data for Isomer **B***: $^1$H NMR: $\delta$ 6.10, 5.88 (2s, 2 x 5H, Cp), 3.10-0.20 (m, 22H, Cy).

**Preparation of [$Mo_2Cp_2(\mu\text{-}PCy_2)(\mu\text{-}\kappa^1\text{:}\eta^2\text{-}HNO)(NO)_2](BF_4)$ (3a)**. Solid $[FeCp_2](BF_4)$ (0.018 g, 0.066 mmol) was added to a dichloromethane solution (10 mL) of compound **1a** (0.040 g, 0.066 mmol), and the mixture was stirred at room temperature for 5 min to give a red solution. After removal of solvent under vacuum, the residue was washed with petroleum ether (4 x 7 mL) to remove ferrocene, then dissolved in dichloromethane and filtered. Removal of solvent from the filtrate yielded compound **3a** as a red solid (0.038 g, 83%). Spectroscopic and microanalytical data for this product were identical to the product obtained from **1a** and $HBF_4{\cdot}OEt_2$ (see reference 11).

**Preparation of [$W_2Cp_2(\mu\text{-}PCy_2)(\mu\text{-}\kappa^1\text{:}\eta^2\text{-}HNO)(NO)_2](BF_4)$ (3b)**. Solid $[FeCp_2](BF_4)$ (0.012 g, 0.044 mmol) was added to a dichloromethane solution (10 mL) of compound **1b** (0.030 g, 0.038 mmol), and the mixture was stirred at room temperature for 5 min to give a brown solution. After removal of solvent under vacuum, the residue was washed with petroleum ether (4 x 7 mL), then dissolved in dichloromethane and filtered. Removal of solvent from the filtrate yielded compound **3b** as a brown solid (0.028 g, 84%). Anal. Calcd for $C_{22}H_{33}BF_4N_3O_3PW_2$: C, 30.27; H, 3.81; N, 4.81. Found: C, 29.95; H, 3.53; N, 4.38. $^1$H NMR: $\delta$ 10.98 (s, br, 1H, NH), 5.85, 5.81 (2s, 2 x 5H, Cp), 2.30-1.00 (m, 22H, Cy).

**Preparation of [$Mo_2Cp_2(\mu\text{-}PCy_2)(\mu\text{-}\kappa^1\text{:}\eta^2\text{-}MeNO)(NO)_2](BAr'_4)$ (4a)**. Solid $[Me_3O](BF_4)$ (0.015 g, 0.101 mmol) was added to a solution of compound **1a** (0.040 g, 0.066 mmol) in dichloromethane (10 mL) at 273 K, and the mixture was stirred at this temperature for 1 h to give a red solution shown by NMR to contain a mixture of the nitroxyl complex **3a** and two isomers of the nitrosomethane complex $[Mo_2Cp_2(\mu\text{-}PCy_2)(\mu\text{-}\kappa^1\text{:}\eta^2\text{-}MeNO)(NO)_2](BF_4)$ (**A**, $\delta_P$ 256.1, and **B**, $\delta_P$ 251.1), in a ratio of ca. 5:6:2 respectively. The solution was then allowed to reach room temperature, then solid $Na(BAr_4')$ (0.059 g, 0.067 mmol) was added, and the mixture stirred for 5 min. The solvent was then removed under vacuum, the residue was extracted with dichloromethane/petroleum ether (1/2) and the extracts were chromatographed on an alumina column at 253 K. Elution with dichloromethane/petroleum ether (1/1) gave a blue fraction containing a small amount of compound **1a**. Elution with dichloromethane/petroleum ether (2/1) gave a rose fraction yielding, after removal of solvents, compound **4a** as a rose solid (0.020 g, 31%). This solid was shown by NMR to contain a mixture of two isomers **A** and **B** in a ratio of ca 2/1. Anal. Calcd for $C_{55}H_{47}BF_{24}Mo_2N_3O_3P$: C, 44.41; H, 3.18; N, 2.82. Found: C, 44.20; H, 3.12; N, 2.67. *Data for isomer **A***: $^1$H NMR: $\delta$ 7.72 (m, 8H, $C_6H_2$), 7.56 (m, 4H, $C_6H_2$), 6.04, 5.75 (2s, 2 x 5H, Cp), 4.00 (d, $J_{PH}$ = 2, 3H, NMe), 2.80-0.60 (m, 22H, Cy). $^{13}C\{^1H\}$ NMR: $\delta$ 162.2 [q, $J_{CB}$ = 50, $C^1(C_6H_2)$], 135.2 [s, $C^2(C_6H_2)$], 129.3 [qq, $J_{CF}$ = 31, $J_{CB}$ = 3, $C^3(C_6H_2)$], 125.0 [q, $J_{CF}$ = 272, $CF_3$], 117.9 [septet, $J_{CF}$ = 3, $C^4(C_6H_2)$], 103.0, 102.8 [2s,

Cp], 68.1 [s, NMe], 50.2 [d, $J_{CP}$ = 13, $C^1$(Cy)], 49.8 [d, $J_{CP}$ = 10, $C^1$(Cy)], 35.1 [d, $J_{CP}$ = 6, $C^2$(Cy)], 35.0 [d, $J_{CP}$ = 5, $2C^2$(Cy)], 34.4 [d, $J_{CP}$ = 2, $C^2$(Cy)], 28.4, 28.3 [d, $J_{CP}$ = 12, $C^3$(Cy)], 28.2 [d, $J_{CP}$ = 13, $C^3$(Cy)], 28.0 [d, $J_{CP}$ = 11, $C^3$(Cy)], 25.8 [s, $2C^4$(Cy)]. *Data for isomer **B***: $^1$H NMR: $\delta$ 6.27, 6.21 (2s, 2 x 5H, Cp), 3.79 (d, $J_{PH}$ = 2, 3H, NMe), 2.80-0.60 (m, 22H, Cy). $^{13}C\{^1H\}$ NMR: $\delta$ 105.1, 102.9 [2s, Cp], 67.3 [s, NMe], 49.5 [d, $J_{CP}$ = 14, $C^1$(Cy)], 43.7 [d, $J_{CP}$ = 11, $C^1$(Cy)], 36.6 [d, $J_{CP}$ = 2, $C^2$(Cy)], 34.6 [d, $J_{CP}$ = 4, $C^2$(Cy)], 33.2 [d, $J_{CP}$ = 6, $C^2$(Cy)], 29.5 [s, $C^2$(Cy)], 28.1 [d, $J_{CP}$ = 17, $2C^3$(Cy)], 27.3 [d, $J_{CP}$ = 11, $C^3$(Cy)], 27.1 [d, $J_{CP}$ = 14, $C^3$(Cy)], 25.8, 25.4 [2s, $C^4$(Cy)].

**Preparation of [$W_2Cp_2(\mu$-$PCy_2)(\mu$-$\kappa^1$:$\eta^2$-MeNO)$(NO)_2$]$(CF_3SO_3)$ (4b)**. Neat $CF_3SO_3Me$ (20 $\mu$L, 0.182 mmol) was added to a solution of compound **1b** (0.015 g, 0.019 mmol) in dichloromethane (10 mL), and the mixture was stirred at room temperature for 5 min to give a cherry red solution. The solvent was then removed under vacuum and the residue was washed with petroleum ether (4 x 5 mL) to yield a cherry red solid shown by NMR to contain a mixture of the nitroxyl complex **3b** ($CF_3SO_3^-$ salt, $\delta_P$ 166.4, $J_{PW}$ = 313, 219) and two isomers (**A** and **B**) of the nitrosomethane complex **4b**, in a ratio of ca. 6:7:2 respectively. Attempts to further purify compound **4b** were unsuccessful. *Data for isomer **A***: $^1$H NMR: $\delta$ 6.28, 6.275 (2s, 2 x 5H, Cp), 4.08 (d, $J_{PH}$ = 1, 3H, NMe), 2.75-1.20 (m, 22H, Cy). *Data for isomer **B***: $^1$H NMR: $\delta$ 6.49, 6.30 (2s, 2 x 5H, Cp), 3.75 (d, $J_{PH}$ = 2, 3H, NMe), 2.75-1.20 (m, 22H, Cy). NMR spectra of the crude reaction mixture can be found in the SI.

**Preparation of [$Mo_2Cp_2(\mu$-$PCy_2)(\mu$-$NH_2)(NO)_2$] (5a)**. A tetrahydrofuran solution (10 mL) of compound **1a** (0.050 g, 0.082 mmol) was stirred vigorously with Na(Hg) (1 mL of a 0.5% amalgam, 1.03 mmol) for 10 min to give a brown solution. The solvent was then removed from the solution under vacuum, the residue was extracted with dichloromethane/petroleum ether (1/2) and the extracts chromatographed on an alumina column at 288 K. Elution with dichloromethane/petroleum ether (2/1) gave a yellow fraction yielding, after removal of solvents, compound **5a** as a yellow solid (0.015 g, 31%). Spectroscopic and microanalytical data for this product were identical to the product obtained from **1a** and Zn(Hg) (see reference 11).

**Preparation of [$W_2Cp_2(\mu$-$PCy_2)(\mu$-$NH_2)(NO)_2$] (5b)**. A tetrahydrofuran solution (10 mL) of compound **1b** (0.030 g, 0.038 mmol) was stirred vigorously with Na(Hg) (1 mL of a 0.5% amalgam, 1.03 mmol) for 5 min to give a yellow solution which was separated from the amalgam by transferring it to an empty Schlenk tube using a canula. The solvent was then removed from the solution under vacuum, the residue was extracted with toluene and the extracts filtered. Removal of solvent from the filtrate gave compound **5b** as a yellow solid (0.010 g, 34%). Anal. Calcd for $C_{22}H_{34}N_3O_2PW_2$: C, 34.26; H, 4.44; N, 5.45. Found: C, 33.95; H, 4.07; N, 5.13. $^1$H NMR: $\delta$ 5.69 (s, 10H, Cp), 3.19 (s, br, 2H, $NH_2$), 2.25-1.10 (m, 22H, Cy).

**Preparation of *cis*-[$Mo_2Cp_2(\mu\text{-}PCy_2)(\mu\text{-}NH_2)(NO)_2$] (*cis*-5a)**. A tetrahydrofuran solution (10 mL) of compound ***cis*-1a** (0.030 g, 0.049 mmol) was stirred vigorously with Na(Hg) (1 mL of a 0.5% amalgam, 1.03 mmol) for 20 min to give a yellow solution. Workup as described for **5a** yielded compound ***cis*-5a** as a yellow solid (0.015 g, 51%). Anal. Calcd for $C_{22}H_{34}Mo_2N_3O_2P$: C, 44.38; H, 5.76; N, 7.06. Found: C, 43.95; H, 5.49; N, 6.84. $\nu$(NH) (Nujol): 3368 (w), 3270 (w); $\nu$(NO) (Nujol): 1578 (vs), 1536 (s). $^1$H NMR: $\delta$ 5.45 (s, 10H, Cp), 3.84, 3.21 (2s, br, 2 x 1H, $NH_2$), 2.45-1.10 (m, 22H, Cy).

**Preparation of [$Mo_2Cp_2(\mu\text{-}PCy_2)\{\mu\text{-}NP(OEt)_3\}(NO)_2$] (6)**. Neat $P(OEt)_3$ (300 $\mu$L, 1.749 mmol) was added to a toluene solution (10 mL) of compound **1a** (0.030 g, 0.049 mmol), and the mixture was refluxed for 20 h to give a yellow solution. After removal of the solvent under vacuum, the residue was extracted with dichloromethane/petroleum ether (1/2) and the extracts chromatographed on an alumina column at 253 K. Elution with dichloromethane/petroleum ether (1/2) gave a yellow fraction yielding, after removal of solvents, essentially pure compound **6** as a yellow oil (0.020 g, 53%). $^{31}P\{^1H\}$ NMR: $\delta$ 215.3 (s, $\mu$-$PCy_2$), 26.9 [s, $\mu$-$NP(OPh)_3$]. $^1$H NMR: $\delta$ 5.59 (s, 10H, Cp), 4.03, 3.83 (2m, 2 x 3H, $OCH_2$), 2.50-1.15 (m, 22H, Cy), 0.98 (t, $J_{HH}$ = 7, 9H, $CH_3$). NMR spectra of this product can be found in the SI.

**Reaction of *cis*-1a with $P(OPh)_3$.** Neat $P(OPh)_3$ (100 $\mu$L, 0.382 mmol) was added to a toluene solution (10 mL) of compound ***cis*-1a** (0.050 g, 0.082 mmol), and the mixture was stirred for 4 days at 344 K to give a yellow solution. After removal of the solvent under vacuum, the residue was extracted with dichloromethane/petroleum ether (1/4) and the extracts were chromatographed on an alumina column at 288 K. Elution with dichloromethane/petroleum ether (1/1) gave a yellow fraction yielding, after removal of solvents, compound *cis*-[$Mo_2Cp_2(\mu\text{-}PCy_2)\{\mu\text{-}NP(OPh)_3\}(NO)_2$] (***cis*-7**) as an oily residue due to the presence of some residual excess $P(OPh)_3$ and $P(O)(OPh)_3$. Further purification was achieved by the slow diffusion of layers of diethyl ether and petroleum ether into a concentrated solution of the above product in toluene. This yielded yellow crystals of ***cis*-7** (0.018 g, 25%). Elution with dichloromethane/petroleum ether (2/1) gave another yellow fraction yielding, after removal of solvents, small amounts of compound ***cis*-5a**. Finally, elution with neat dichloromethane gave a purple fraction yielding, after removal of solvent, an uncharacterized product identified by singlet $^{31}P\{^1H\}$ NMR resonances at 234.3 and 108.4 ppm, and N–O stretches at 1620 (w) and 1596 (vs) $cm^{-1}$, as a red solid (0.006 g, 7%). Attempts to grow single crystals of this product suitable for an X-ray diffraction study were unsuccessful. *Data for compound **cis*-7***: Anal. Calcd for $C_{40}H_{47}Mo_2N_3O_5P_2$: C, 53.17; H, 5.24; N, 4.65. Found: C, 53.35; H, 5.57; N, 4.45. $^{31}P\{^1H\}$ NMR: $\delta$ 223.0 (s, $\mu$-$PCy_2$), –2.3 [s, $\mu$-$NP(OPh)_3$]. $^1$H NMR: $\delta$ 7.40-7.10 (m, 15H, Ph), 5.32 (s, 10H, Cp), 2.50-1.10 (m, 22H, Cy).

**X-Ray Structure Determination of Compound *cis*-1a.** X-ray intensity data for this compound were collected on a Kappa-Appex-II Bruker diffractometer using graphite-monochromated MoK$_\alpha$ radiation at 100 K. The software APEX[42] was used for collecting frames with $\omega/\phi$ scans measurement method. Twinning was found to occur in the crystal. The experimental data were treated as two domain twinned data, the second domain being rotated from the first one by 179.9 degrees about reciprocal axis 1.000 0.054 0.058 and real axis 1.000 –0.001 0.000. The program Cell Now[43] was used to determine the twin law, the cell dimensions and orientation matrixes. The Bruker SAINT software was used for the data reduction,[44] and a multi-scan absorption correction was applied with TWINABS.[45] Using the program suite WINGX,[46] the structure was solved by Patterson interpretation and phase expansion using SIR92,[47] and refined with full-matrix least squares on $F^2$ using SHELXL2016.[48] Two independent molecules of the complex, very similar one to each other, were present in the asymmetric unit. Positional parameters and anisotropic temperature factors for all non-H atoms were refined anisotropically, and all hydrogen atoms were geometrically placed and refined using a riding model.

**X-Ray Structure Determination of Compound 1b.** Data collection for this compound was performed at 153 K on an Oxford Diffraction Xcalibur Nova single crystal diffractometer, using Cu Kα radiation. Images were collected at a 62 mm fixed crystal-detector distance using the oscillation method, with 1º oscillation and variable exposure time per image (60-250 s). Data collection strategy was calculated with the program *CrysAlis Pro CCD*,[49] and data reduction and cell refinement was performed with the program *CrysAlis Pro RED*.[49] An empirical absorption correction was applied using the SCALE3 ABSPACK algorithm as implemented in the program *CrysAlis Pro RED*. The structures were solved and refined as described for ***cis*-1a**, but using SHELXL2016.[48] Twinning was found to occur in the crystal, but the twin law could not be determined. Moreover both cyclopentadienyl and cyclohexyl groups were disordered in each case. Disorder in the cyclopentadienyl groups was satisfactorily modeled over two sites with occupancy factors of 0.6/0.40 and 0.5/0.5 respectively. However, the slight disorder present in the cyclohexyl groups could not be satisfactorily modeled, so it remained unsolved. Due to the poor quality of the diffraction data, not all non-H atoms could be refined anisotropically; a few of them had to be refined anisotropically in combination with the instructions DELU and SIMU, while the bridging N(3) atom and the disordered cyclopentadienyl carbon atoms were refined isotropically to prevent their temperature factors from becoming non-positive definite. All hydrogen atoms were geometrically placed and refined using a riding model. Upon convergence, the strongest residual peaks were placed around the W atom.

**Computational Details**. All DFT calculations were carried out using the GAUSSIAN03 package,[50] in which the hybrid method B3LYP was used with the Becke three-parameter exchange functional,[51] and the Lee-Yang-Parr correlation functional.[52] A pruned numerical integration grid (99,590) was used for all the calculations *via* the keyword Int=Ultrafine. Effective core potentials and their associated double-ζ LANL2DZ basis set were used for Mo and W atoms.[53] The light elements (P, N, O, C and H) were described with the 6-31G* basis.[54] Geometry optimizations were performed under no symmetry restrictions, using initial coordinates derived from the X-ray data. Frequency analyses were performed for all the stationary points to ensure that a minimum structure with no imaginary frequencies was achieved. Molecular orbitals and vibrational modes were visualized using the MOLEKEL program.[55]

**Table 4.** Crystal Data for New Compounds

| | ***cis*-1a** | **1b** |
|---|---|---|
| mol formula | $C_{22}H_{32}Mo_2N_3O_3P$ | $C_{22}H_{32}N_3O_3PW_2$ |
| mol wt | 609.35 | 785.17 |
| cryst syst | Triclinic | Monoclicnic |
| space group | *P*–1 | $P2_1/c$ |
| radiation ($\lambda$, Å) | 0.71073 | 1.54184 |
| *a*, Å | 10.2830(4) | 16.248(5) |
| *b*, Å | 14.7143(7) | 10.249(5) |
| *c*, Å | 16.3523(7) | 14.267(5) |
| $\alpha$, deg | 77.972(3) | 90 |
| $\beta$, deg | 87.897(2) | 94.663(5) |
| $\gamma$, deg | 87.711(2) | 90 |
| *V*, Å$^3$ | 2416.95(18) | 2368.0(16) |
| Z | 4 | 4 |
| calcd density, g cm$^{-3}$ | 1.675 | 2.202 |
| absorp coeff, mm$^{-1}$ | 1.132 | 18.566 |
| temperature, K | 100.0(1) | 153(5) |
| $\theta$ range (deg) | 1.27-30.63 | 5.11-69.64 |
| index ranges (*h*, *k*, *l*) | –14, 14; –21, 21; –23, 23 | –19, 17; –12, 12; –13, 17 |
| no. of reflns collected | 149022 | 10458 |
| no. of indep reflns ($R_{int}$) | 149022 | 4366 (0.1518) |
| reflns with $I > 2\sigma(I)$ | 101666 | 2234 |
| *R* indexes [data with $I > 2\sigma(I)$][a] | $R_1$ = 0.0518 w$R_2$ = 0.1016[b] | $R_1$ = 0.1140 w$R_2$ = 0.2804[c] |
| *R* indexes (all data)[a] | $R_1$ = 0.0925 w$R_2$ = 0.1164[b] | $R_1$ = 0.1762 w$R_2$ = 0.3743[c] |
| GOF | 0.996 | 1.054 |
| no. of restraints/params | 0 / 560 | 122 / 229 |
| $\Delta\rho$(max., min.), eÅ$^{-3}$ | 1.738 / –1.037 | 2.745 / –3.356 |
| CCDC deposition no | 1859488 | 1859489 |

[a] $R = \Sigma||F_o| - |F_c|| / \Sigma|F_o|$. $wR = [\Sigma w(|F_o|^2 - |F_c|^2)^2 / \Sigma w|F_o|^2]^{1/2}$. $w = 1/[\sigma^2(F_o^2) + (aP)^2 + bP]$ where $P = (F_o^2 + 2F_c^2)/3$. [b] $a$ = 0.0412, $b$ = 0.0000. [c] $a$ = 0.1915, $b$ = 0.0000.

**Supporting Information.** A PDF file containing results of DFT calculations (structures, energies, atomic charges, and IR data) and NMR spectra for compounds **4b** and **6**, and an XYZ file including the Cartesian coordinates for all computed species. This material is available free of charge *via* the Internet at http://pubs.acs.org.

**Author Information.** Corresponding authors: E-mail: garciavdaniel@uniovi.es (D. G. V.), mara@uniovi.es (M. A. R).

**Acknowledgment.** We thank the Gobierno del Principado de Asturias for a grant (to A. T.) and financial support (Project GRUPIN14-011), the MINECO of Spain and FEDER for financial support (Project CTQ2015-63726-P), the CMC of the Universidad de Oviedo for access to computing facilities, and the X-Ray units of the Universities of Oviedo and Santiago de Compostela for acquisition of diffraction data.

## References

1. (a) Richter-Addo, G. B.; Legzdins, P. *Metal Nitrosyls*; Oxford University Press: Oxford, U. K., 1992. (b) Mingos, D. M. P. (Ed.), Nitrosyl Complexes in Inorganic Chemistry, Biochemistry and Medicine; *Struct. Bond.* **2014**, Vols 153 and 154.
2. For some recent reviews, see: (a) Hunt, A. P.; Lehnert, N. Heme-Nitrosyls: Electronic Structure Implications for Function in Biology. *Acc. Chem. Res.* **2015**, *48*, 2117-2125. (b) Tsai, M. L.; Tsou, C. C.; Liaw, W. F. Dinitrosyl Iron Complexes (DNICs): From Biomimetic Synthesis and Spectroscopic Characterization toward Unveiling the Biological and Catalytic Roles of DNICs. *Acc. Chem. Res.* **2015**, *48*, 1184-1193. (c) Tram, C. T.; Skodje, K. M.; Kim, E. Monomeric Dinitrosyl Iron Complexes: Synthesis and Reactivity. *Progr. Inorg. Chem.* **2014**, *59*, 339-380. (d) Doctorovich, F.; Bikiel, D. E.; Pellegrino, J.; Suarez, S. A.; Marti, M. A. Reactions of HNO with Metal Porphyrins: Underscoring the Biological relevance of HNO. *Acc. Chem. Res.* **2014**, *47*, 2907-2916. (e) Franke, A.; van Eldik, R. Factors that Determine the Mechanism of NO Activation by Metal Complexes of Biological and Environmental Relevance. *Eur. J. Inorg. Chem.* **2013**, 460-480. (f) Berto, T. C.; Speelman, A. M.; Zheng, S.; Lehnert, N. Mono- and dinuclear non-heme iron–nitrosyl complexes: Models for key intermediates in bacterial nitric oxide reductases. *Coord. Chem. Rev.* **2013**, *257*, 244-259.
3. Xiang, H. J.; Guo, M.; Liu, J. G. Transition-Metal Nitrosyls for Photocontrolled Nitric Oxide Delivery. *Eur. J. Inorg. Chem.* **2017**, *12*, 1586-1595.
4. (a) *Reduction of Nitrogen Oxide Emissions*; Ozkan, U. S.; Agarwal, S. K.; Marcelin, G., Eds.; American Chemical Society: Washington, DC, 1995. (b) *Environmental Catalysis*; Armor, J. M., Ed.; American Chemical Society: Washington, DC, 1994. (c) *Catalytic Control of Air Pollution*; Silver, R. G.; Sawyer, J. E.; Summers, J. C., Eds.; American Chemical Society: Washington, DC 1992. (d) *Energy and the Environment*; Dunderdale, J., Ed.; Royal Society of Chemistry: Cambridge, U. K., 1990. (e) *Pollution: Causes, Effects and Control*; Harrison, R. M., Ed.; Royal Society of Chemistry: Cambridge, U. K., 1990.
5. (a) Lai, J.-K.; Wachs, I. E. A Perspective on the Selective Catalytic Reduction (SCR) of NO with $NH_3$ by Supported $V_2O_5$–$WO_3$/$TiO_2$ Catalysts. *ACS Catal.* **2018**, *8*, 6537-6551. (b) Liu, Y.; Zhao, J.; Lee, J.-M. Conventional and New Materials for

Selective Catalytic Reduction (SCR) of $NO_x$. *ChemCatChem* **2018**, *10*, 1499-1511. (c) Liu, F.; Yu, Y.; He, H. Environmentally-benign catalysts for the selective catalytic reduction of $NO_x$ from diesel engines: structure-activity relationships and reaction mechanism aspects. *Chem. Commun.* **2014**, *50*, 8445-8463. (d) Granger, P.; Parvulescu, V. I. Catalytic $NO_x$ Abatement Systems for Mobile Sources: From Three-Way to Lean Burn after-Treatment Technologies. *Chem. Rev.* **2011**, *111*, 3155-3207.

6. Legzdins, P.; Young, M. A.; Batchelor, R. J.; Einstein, F. W. B. Spontaneous Isomerization of Symmetric M(μ-NO)$_2$M Linkages to (ON)M:N:M:O Groupings. *J. Am. Chem. Soc.* **1995**, *117*, 8798-8806.
7. (a) Hames, B. W.; Legzdins, P.; Oxley, J. C. Organometallic nitrosyl chemistry. 13. Reactions of sodium dihydridobis(2-methoxyethoxy)aluminate with some cationic and neutral nitrosyl complexes. *Inorg. Chem.* **1980**, *19*, 1565-1571. (b) Ball, R. G.; Hames, B. W.; Legzdins, P.; Trotter, J. Organometallic nitrosyl chemistry. 14. Novel reactivity of $LiEt_3BH$ with $[(\eta^5\text{-}C_5H_5)Cr(NO)_2]_2$: conversion of a bridging nitrosyl ligand to a bridging $EtNBEt_2$ group. *Inorg. Chem.* **1980**, *19*, 3626-3631. (c) Müller, J.; Sonn, I.; Strampfer, M. Reaktionen von Nitrosylkomplexen: XI. Überführung von μ-NO- in μ-$NH_2$-Liganden durch katalytische Hydrierung am Beispiel von $[Cp'Co(\mu\text{-}NO)]_2$ sowie von $[CpCr(\mu\text{-}NO)NO]_2$. *J. Organomet. Chem.* **1992**, *427*, C15-C18.
8. (a) Böttcher, H.-C.; Graf, M.; Mereiter, K.; Kirchner, K. Reductive Dimerization of Nitric Oxide to *trans*-Hyponitrite in the Coordination Sphere of a Dinuclear Ruthenium Complex. *Organometallics* **2004**, *23*, 1269-1273. (b) Böttcher, H.-C.; Wagner, C; Kirchner, K. Reaction Properties of the trans-Hyponitrite Complex $[Ru_2(CO)_4(\mu\text{-}H)(\mu\text{-}PBu^t_2)(\mu\text{-}Ph_2PCH_2PPh_2)(\mu\text{-}\eta^2\text{-}ONNO)]$. *Inorg. Chem.* **2004**, *43*, 6294-6299. (c) Arikawa, Y.; Asayama, T.; Moriguchi, M.; Agari, S.; Onishi, M. Reversible N−N Coupling of NO Ligands on Dinuclear Ruthenium Complexes and Subsequent $N_2O$ Evolution: Relevance to Nitric Oxide Reductase. *J. Am. Chem. Soc.* **2007**, *129*, 14160-14161. (d) Suzuki, T.; Tanaka, H.; Shiota, Y.; Sajith, P. K.; Arikawa, Y.; Yoshizawa, K. Proton-Assisted Mechanism of NO Reduction on a Dinuclear Ruthenium Complex. *Inorg. Chem.* **2015**, *54*, 7181-7191.
9. Arikawa, Y.; Hiura, J.; Tsuchii, C.; Kodama, M.; Matsumoto, N.; Umakoshi, K. Synthetic NO reduction cycle on a bis(pyrazolato)-bridged dinuclear ruthenium complex including photo-induced transformation. *Dalton Trans.* **2018**, *47*, 7399-7401.
10. (a) Legzdins, P.; Nurse, C.; Rettig, S. J. Organometallic nitrosyl chemistry. 18. Electrophile-induced reduction of coordinated nitrogen monoxide. Sequential conversion of a $\mu_3$-nitrosyl group to $\mu_3$-hydroxylimido and $\mu_3$-imido ligands by

protonic acids. *J. Am. Chem. Soc.* **1983**, *105*, 3727-3728. (b) Fjare, D. E.; Gladfelter, W. L. Deoxygenation of a cluster-coordinated nitric oxide. *J. Am. Chem. Soc.* **1984**, *106*, 4799-4810. (c) Johnson, B. F. G.; Lewis, J.; Mace, J. M. The reduction of ($\mu_2$-NO) in [$HRu_3(CO)_{10}(\mu_2$-NO)] to ($\mu_3$-NH) and ($\mu_2$-$NH_2$) by molecular hydrogen. *J. Chem. Soc., Chem. Commun.* **1984**, 186-188. (d) Smieja, J. A.; Stevens, R. E.; Fjare, D. E.; Gladfelter, W. L. Nitrogen-oxygen bond cleavage of cluster-coordinated nitric oxide ligands using molecular hydrogen. *Inorg. Chem.* **1985**, *24*, 3206-3213. (e) Smieja, J. A.; Gladfelter, W. L. The reduction of cluster-coordinated nitric oxide using molecular hydrogen. Synthesis and characterization of $H_4Os_3(NH)(CO)_8$. *J. Organomet. Chem.* **1985**, *297*, 349-359.

11. Alvarez, M. A.; García, M. E.; García-Vivó, D.; Ruiz, M. A.; Toyos, A. Mild N–O Bond Cleavage Reactions of a Pyramidalized Nitrosyl Ligand Bridging a Dimolybdenum Center. *Inorg. Chem.* **2015**, *54*, 10536-10538.
12. Alvarez, M. A.; García, M. E.; Martínez, M. E.; Ramos, A.; Ruiz, M. A. Migration and Insertion Processes in the Reactions of the Hydrocarbyl-Bridged Unsaturated Complexes [$Mo_2(\eta^5$-$C_5H_5)_2(\mu$-R)($\mu$-$PCy_2$)$(CO)_2$] (R= Me, $CH_2Ph$, Ph) with CO and NO. *Organometallics* **2009**, *28*, 6293-6307.
13. Alvarez, M. A.; García, M. E.; García-Vivó, D.; Melón, S.; Ruiz, M. A.; Toyos, A. Reactions of the Unsaturated Ditungsten Complexes [$W_2Cp_2(\mu$-$PPh_2)_2(CO)_x$] (x = 1, 2) with Nitric Oxide. Stereoselective Carbonyl Displacement and Oxygen-Transfer Reactions of a Nitrite Ligand. *Inorg. Chem.* **2014**, *53*, 4739-4750.
14. García, M. E.; Riera, V.; Ruiz, M. A.; Rueda, M. T.; Sáez, D. Dimolybdenum and tungsten cyclopentadienyl carbonyls with electron-rich phosphido bridges. Synthesis of hydridophosphido [$M_2Cp_2(\mu$-H)($\mu$-PRR´)$(CO)_4$] and unsaturated bisphosphido complexes [$M_2Cp_2(\mu$-$PR_2)(\mu$-PR´R´´)$(CO)_x$] (x=1, 2; R, R´, R´´= Et, Cy, $^t$Bu). *Organometallics* **2002**, *21*, 5515-5525.
15. The $PPh_2$-bridged complexes analogous to compounds **2a** and **2b** were prepared independently by us through the reaction of the nitrosyl complexes [$M_2Cp_2(\mu$-$PPh_2)(CO)_3(NO)$] with $[NO]BF_4$, and they display similar spectroscopic properties (García, M. E.; Rueda, M. T.; Ruiz, M. A., unpublished results). The structure of the symmetrical isomer **A** of the $Mo_2$ complex was determined crystallographically and the corresponding data are deposited at the CCDC (no. 1867401).
16. One-bond P–M couplings are particularly sensitive to the nature of the M-bound ligand positioned *trans* to the P atom, and also to the coordination number of M. See Jameson, C. J. In *Phosphorus-31 NMR Spectroscopy in Stereochemical Analysis*; Verkade, J. G., Quin, L. D., Eds.; VCH: Deerfield Beach, FL, 1987; Chapter 6.

17. Alvarez, M. A.; García, M. E.; García-Vivó, D.; Ruiz, M. A.; Toyos, A. E–H Bond Activation and Insertion Processes in the Reactions of the Unsaturated Hydride $[W_2Cp_2(\mu\text{-}H)(\mu\text{-}PPh_2)(NO)_2]$. *Inorg. Chem.* **2018**, *57*, 2228-2241.
18. In a regular tetrahedral distribution of atoms or electron pairs (X) around a central atom (A), the X–A–X angle is ca. 109.5º, then the $\alpha$ angle mentioned in Table 2 can be calculated as $\alpha$ =1/2(360-109.5) = 125.25º.
19. (a) Johnson, B. F. G.; Lewis, J.; Mace, J. M.; Raithby, P. R.; Stevens, R. E.; Gladfelter, W. L. Decacarbonylnitrosyltriosmate(3 Os-Os)(1-): structural analysis and fluxional properties. *Inorg. Chem.* **1984**, *23*, 1600-1603. (b) Müller, J.; Mansoni de Oliveira, G.; Pickardt, J. Reaktionen von Nitrosylkomplexes: VII. Bildung von μ-Amido-Liganden Durch Carbanion-Addition an oder katalytische Hydrierung von μ-Nitrosyl-Liganden. *J. Organomet. Chem.* **1987**, *329*, 241-250. (c) Varonka, M. S.; Warren, T. H. Three-Coordinate N-Heterocyclic Carbene Nickel Nitrosyl Complexes. *Organometallics* **2010**, *29*, 717-720. (d) Mayer, T.; Mayer, P.; Böttcher, H.-C. Diazald: An entry to diruthenium complexes containing bridging nitrosyl ligands. *J. Organomet. Chem.* **2014**, *751*, 368-373.
20. Kubat-Martin, K. A.; Barr, M. E.; Spencer, B.; Dahl, L. F. Stereochemical and Electrochemical Characterization of the Iron-Iron Multiple-Bonded $[Fe_2(\eta^5\text{-}C_5H_{5-x}Me_x)_2(\mu\text{-}NO)_2]^n$ Dimers (x = 0, 1, 5; n = 0, 1–): a Structural-Bonding Analysis of the Iron and Cobalt Nitrosyl Bridged $[M_2(\eta^5\text{-}C_5H_5)_2(\mu\text{-}NO)_2]^n$ Series (M = Fe, n = 0, 1–; M = Co, n = 1+, 0). *Organometallics* **1987**, *6*, 2570-2579.
21. Mayer, T.; Böttcher, H.-C. Protonation of metal–metal bonds in nitrosyl-bridged diruthenium complexes. *Polyhedron* **2014**, *69*, 240-243.
22. Braterman, P. S. *Metal Carbonyl Spectra*; Academic Press: London, U. K., 1975.
23. De la Cruz, C.; Sheppard, N. A structure-based analysis of the vibrational spectra of nitrosyl ligands in transition-metal coordination complexes and clusters. *Spectrochim. Acta, Part A* **2011**, *78*, 7-28.
24. (a) Cramer, C. J. *Essentials of Computational Chemistry, 2nd Ed.*; Wiley: Chichester, UK, 2004. (b) Koch, W.; Holthausen, M. C. *A Chemist´s Guide to Density Functional Theory, 2nd Ed.*; Wiley-VCH: Weinheim, 2002.
25. Alvarez, M. A.; García, M. E.; García-Vivó, D.; Ruiz, M. A.; Toyos, A. The Doubly-Bonded Ditungsten Anion $[W_2Cp_2(\mu\text{-}PPh_2)(NO)_2]^-$: An Entry to the Chemistry of Unsaturated Nitrosyl Complexes. *Dalton Trans.* **2016**, *45*, 13300-13303.
26. (a) Connelly, N. G. Synthetic applications of Organotransition-metal Redox Reactions. *Chem. Soc. Rev.* **1989**, *18*, 153-185. (b) Sun, S.; Sweigart, D. A. Reactions of 17- and 19-Electron Organometallic Complexes. *Adv. Organomet. Chem.* **1996**, *40*, 171-214. c) Geiger, W. E. Organometallic Electrochemistry:

Origins, Development and Future. *Organometallics* **2007**, *26*, 5738-5765. d) Pombeiro, A. J. L.; Guedes da Silva, M. F. C.; Lemos, M. A. N. D. A. Electron-transfer induced isomerizations of coordination compounds. *Coord. Chem. Rev.* **2001**, *219-221*, 53-80.

27. (a) Melenkivitz, R.; Hillhouse, G. L. Synthesis, structure, and reactions of a nitroxyl complex of iridium(III), *cis*,*trans*-$IrHCl_2(NH{=}O)(PPh_3)_2$. *Chem. Commun.* **2002**, 660-661. (b) Sellmann, D.; Gottschalk-Gaudig, T.; Haubinger, D.; Heinemann, F. W.; Hess, B. A. [Ru(HNO)(′pybuS4′)], the First HNO Complex Resulting from Hydride Addition to a NO Complex (′pybuS4′2−=2,6-Bis(2-mercapto-3,5-di-tert-butylphenylthio)dimethylpyridine(2−). *Chem. Eur. J.* **2001**, *7*, 2099-2103. (c) Wilson, R. D.; Ibers, J. A. Coordinated nitrosyl hydride: structural and spectroscopic study of dichlorocarbonyl(nitrosyl hydride)bis(triphenylphosphine)osmium(II). *Inorg. Chem.* **1979**, *18*, 336- 343.
28. (a) Wiese, S.; Kapoor, P.; Williams, K. D.; Warren, T. H. Nitric Oxide Oxidatively Nitrosylates Ni(I) and Cu(I) C-Organonitroso Adducts. *J. Am. Chem. Soc.* **2009**, *131*, 18105-18111. (b) O´Connor, J. M.; Bunker, K. D. Conversion of ($\eta^5$-$C_5H_5$)$Co(PPh_3)_2$ and Nitro Compounds to Mononuclear $\eta^1$(*N*)-Nitrosoalkyl and Dinuclear μ-$\eta^1$(*N*):$\eta^2$(*N*,*O*)-Nitrosoaryl Complexes. *Organometallics* **2003**, *22*, 5268-5273. (c) Hoard, D. W.; Sharp, P. R. Chemistry of [Cp*Rh($\mu$-Cl)]$_2$ and its Dioxygen and Nitrosobenzene Insertion Products. *Inorg. Chem.* **1993**, *32*, 612-620. (d) Stella, S.; Floriani, C.; Chiesi-Villa, A.; Guastini, C. Side-on bonded nitrosobenzene bridging two metal atoms, in a binuclear cyclopentadienyl cobalt complex: crystal structure of [{Co(cp)}$_2$(μ-$PhNO)_2$]. *J. Chem. Soc. Dalton Trans.* **1988**, 545-547. (e) Barrow, M. J.; Mills, O. S. Carbon compounds of the transition metals. Part XXI. The crystal and molecular structure of bis[tricarbonyl-(3-chloro-2-methylnitrosobenzene)iron]. *J. Chem. Soc. A* **1971**, 864-868.
29. Kramarz, K. W.; Norton, J. R. Slow Proton-Transfer Reactions in Organometallic and Bioinorganic Chemistry. *Progr. Inorg. Chem.* **1994**, *42*, 1-65.
30. García, M. E.; Melón, S.; Ruiz, M. A.; Marchiò, L.; Tiripicchio, A. Nitrosyl derivatives of the unsaturated dihydrides [$Mn_2$(μ-$H)_2(CO)_6$(μ-$L_2$)] ($L_2$ = $Ph_2PCH_2PPh_2$, $(EtO)_2POP(OEt)_2$). *J. Organomet. Chem.* **2011**, *696*, 559-567.
31. (a) Alvarez, M. A.; García, M. E.; Ramos, A.; Ruiz, M. A.; Lanfranchi, M.; Tiripicchio, A. Alkenyl Derivatives of the Unsaturated Dimolybdenum Hydride Complex [$Mo_2$($\eta^5$-$C_5H_5)_2$($\mu$-H)($\mu$-$PCy_2$)$(CO)_2$]. *Organometallics* **2007**, *26*, 5454-5467. (b) Alvarez, M. A.; García, M. E.; García-Vivó, D.; Ruiz, M. A.; Vega, M. F. Insertion and C–C Coupling Processes in Reactions of the Unsaturated Hydride [$W_2Cp_2$(H)($\mu$-$PCy_2$)$(CO)_2$] with Alkynes. *Dalton Trans.* **2016**, *45*, 5274-5289.

32. Schollhammer, P.; Petillon, F. Y.; Poder-Guillou, S.; Saillard, J. Y.; Talarmin, J.; Muir K. W. Disproportionation of hydrazine by $[Mo_2(\eta\text{-}C_5H_5)_2(\mu\text{-}Cl)(\mu\text{-}SMe)_3]$ and formation of an $Mo_2(\mu\text{-}NH_2)$ amido bridge. *Chem. Commun.* **1996**, 2633-2634.
33. One-bond P–W couplings in complexes *trans*-$[W_2Cp_2(\mu\text{-}PPh_2)(\mu\text{-}X)(NO)_2]$ increase linearly with the Pauling electronegativity ($\chi_P$) of the bridgehead atom of X, according to the equation $J_{PW} = 253 + 42\chi_P$ (see reference 17). This gives an expected value of 381 Hz when X = N, therefore some 360 Hz if considering a related $PCy_2$-bridged complex.
34. Scepaniak, J. J.; Margarit, C. G.; Harvey, J. N.; Smith, J. M. Nitrogen Atom Transfer from Iron(IV) Nitrido Complexes: A Dual-Nature Transition State for Atom Transfer. *Inorg. Chem.* **2011**, *50*, 9508-9517.
35. Pyykkö, P.; Atsumi, M. Molecular Double-Bond Covalent Radii for Elements Li-E112. *Chem. Eur. J.* **2009**, *15*, 12770-12779.
36. Range of distances according to a search on the Cambridge Crystallographic Data Centre database (updated August 2018). The search yielded some 40 complexes with $\mu$-N=$PX_3$ ligands having X = alkyl or aryl, but just two complexes with X = $NR_2$ ($\mu$-N–P = 1.54 and 1.58 Å respectively); see: (a) Robinson, T. P.; Price, R. D.; Davidson, M. G.; Fox, M. A.; Johnson, A. L. Why are the $\{Cu_4N_4\}$ rings in copper(I) phosphinimide clusters $[Cu\{\mu\text{-}N{=}PR_3\}]_4$ (R = $NMe_2$ or Ph) planar?. *Dalton Trans.* **2015**, *44*, 5611-5619. (b) Riese, U.; Harms, K.; Pebler, J.; Dehnicke, K. Phosphaniminato-Cluster von Eisen. Die Kristallstrukturen von $[FeCl(NPEt_3)]_4$, $[Fe(C{=}C\text{–}SiMe_3)(NPEt_3)]_4$ und $[Fe_3Cl_4\{NP(NMe_2)_3\}_3]$. *Z. Anorg. Allg. Chem.* **1999**, *625*, 746-754.
37. Arikawa, Y.; Otsubo, Y.; Fujino, H.; Horiuchi, S.; Sakuda, E.; Umakoshi, K. Nitrite Reduction Cycle on a Dinuclear Ruthenium Complex Producing Ammonia. *J. Am. Chem. Soc.* **2018**, *140*, 842-847.
38. Cui, P.; Wang, Q.; McCollom, S. P.; Manor, B. C.; Carroll, P. J.; Tomson, N. C. Ring-Size Modulated Reactivity of Putative Dicobalt-Bridging Nitrides: C–H Activation versus Phosphinimide Formation. *Angew. Chem. Int. Ed.* **2017**, *56*, 15979-15983.
39. Armarego, W. L. F.; Chai, C. *Purification of Laboratory Chemicals, 7th ed.*; Butterworth-Heinemann: Oxford, U. K, 2012.
40. Connelly, N. G.; Geiger, W. E. Chemical Redox Agents for Organometallic Chemistry. *Chem. Rev.* **1996**, *96*, 877-910.
41. Yakelis, N. A.; Bergman, R. G. Safe Preparation and Purification of Sodium Tetrakis[(3,5-trifluoromethyl)phenyl]borate ($NaBArF_{24}$): Reliable and Sensitive Analysis of Water in Solutions of Fluorinated Tetraarylborates. *Organometallics* **2005**, *24*, 3579-3581.

42. *APEX 2, version 2.0-1*, Bruker AXS Inc: Madison, WI, 2005.
43. Sheldrick, G. M. *Cell Now, version 2008/2*, University of Göttingen: Göttingen, Germany, 2008.
44. *SMART & SAINT Software Reference Manuals, Version 5.051*; Bruker AXS Inc: Madison WI, 1998.
45. *TWINABS*, Bruker AXS Inc: Madison, WI, 2001.
46. Farrugia, L. J. WinGX suite for small-molecule single-crystal crystallography. *J. Appl. Crystallogr.* **1999**, *32*, 837-838.
47. Altomare, A.; Cascarano, G.; Giacovazzo, C.; Guagliardi, A.; Burla, M. C.; Polidori, G.; Camalli, M. SIR92 - a program for automatic solution of crystal structures by direct methods. *J. Appl. Crystallogr.* **1994**, *27*, 435-435.
48. (a) Sheldrick, G. M. A short history of SHELX. *Acta Crystallogr., Sect. A* **2008**, *64*, 112-122. (b) Sheldrick, G. M. Crystal structure refinement with SHELXL. *Acta Crystallogr., Sect. C* **2015**, *71*, 5-8.
49. *CrysAlis Pro*; Oxford Diffraction Limited, Ltd.: Oxford, U. K., 2006.
50. Frisch, M. J.; Trucks, G. W.; Schlegel, H. B.; Scuseria, G. E.; Robb, M. A.; Cheeseman, J. R.; Montgomery, Jr., J. A.; Vreven, T.; Kudin, K. N.; Burant, J. C.; Millam, J. M.; Iyengar, S. S.; Tomasi, J.; Barone, V.; Mennucci, B.; Cossi, M.; Scalmani, G.; Rega, N.; Petersson, G. A.; Nakatsuji, H.; Hada, M.; Ehara, M.; Toyota, K.; Fukuda, R.; Hasegawa, J.; Ishida, M.; Nakajima, T.; Honda, Y.; Kitao, O.; Nakai, H.; Klene, M.; Li, X.; Knox, J. E.; Hratchian, H. P.; Cross, J. B.; Bakken, V.; Adamo, C.; Jaramillo, J.; Gomperts, R.; Stratmann, R. E.; Yazyev, O.; Austin, A. J.; Cammi, R.; Pomelli, C.; Ochterski, J. W.; Ayala, P. Y.; Morokuma, K.; Voth, G. A.; Salvador, P.; Dannenberg, J. J.; Zakrzewski, V. G.; Dapprich, S.; Daniels, A. D.; Strain, M. C.; Farkas, O.; Malick, D. K.; Rabuck, A. D.; Raghavachari, K.; Foresman, J. B.; Ortiz, J. V.; Cui, Q.; Baboul, A. G.; Clifford, S.; Cioslowski, J.; Stefanov, B. B.; Liu, G.; Liashenko, A.; Piskorz, P.; Komaromi, I.; Martin, R. L.; Fox, D. J.; Keith, T.; Al-Laham, M. A.; Peng, C. Y.; Nanayakkara, A.; Challacombe, M.; Gill, P. M. W.; Johnson, B.; Chen, W.; Wong, M. W.; Gonzalez, C.; and Pople, J. A.; *Gaussian 03, Revision B.02*; Gaussian, Inc.: Wallingford, CT, 2004.
51. Becke, A. D. Density-functional thermochemistry. III. The role of exact exchange. *J. Chem. Phys.* **1993**, *98*, 5648-5652.
52. Lee, C.; Yang, W.; Parr, R. G. Development of the Colle-Salvetti correlation-energy formula into a functional of the electron density. *Phys. Rev. B* **1988**, *37*, 785-789.

53. Hay, P. J.; Wadt, W. R. Ab initio effective core potentials for molecular calculations. Potentials for potassium to gold including the outermost core orbitals. *J. Chem. Phys.* **1985**, *82*, 299-310.
54. (a) Hariharan, P. C.; Pople, J. A. Influence of polarization functions on MO hydrogenation energies. *Theor. Chim. Acta* **1973**, *28*, 213-222. (b) Petersson, G. A.; Al-Laham, M. A. A complete basis set model chemistry. II. Open-shell systems and the total energies of the first-row atoms. *J. Chem. Phys.* **1991**, *94*, 6081-6090. (c) Petersson, G. A.; Bennett, A.; Tensfeldt, T. G.; Al-Laham, M. A.; Shirley, W. A.; Mantzaris, J. A complete basis set model chemistry. I. The total energies of closed-shell atoms and hydrides of the first-row elements. *J. Chem. Phys.* **1988**, *89*, 2193-2218.
55. Portmann, S.; Luthi, H. P. MOLEKEL: An Interactive Molecular Graphics Tool. *CHIMIA* **2000**, *54*, 766-770.

# (For Table of Contents Use Only)

## Table of Contents Synopsis

The bridging NO in the title complexes displays significant pyramidalization at the N atom, which can be protonated or methylated to give nitroxyl or nitromethane derivatives. Electron releasing reagents or O-acceptor molecules trigger full N–O bond cleavage in this ligand to eventually yield amido- or phosphoraniminato-bridged derivatives.

## Graphics for Table of Contents